



Regulation of heat transfer in Rayleigh–Bénard convection in Newtonian liquids and Newtonian nanoliquids using gravity, boundary temperature and rotational modulations

C. Kanchana¹ · P. G. Siddheshwar² · Yi Zhao¹

Received: 20 September 2019 / Accepted: 11 January 2020 / Published online: 3 February 2020
© Akadémiai Kiadó, Budapest, Hungary 2020

Abstract

The individual effect of time-periodic gravity modulation, in-phase and out-of-phase temperature modulations and rotational modulation on Rayleigh–Bénard convection in twenty-eight nanoliquids is studied in the paper using the two-phase description of the generalized Buongiorno model. The generalized Lorenz model for each modulation problem is derived using the truncated Fourier series representation. The method of multiscales is employed to arrive at the Ginzburg–Landau equations from the Lorenz models, and the solution of Ginzburg–Landau equations is used to quantify the heat transport. The modulation amplitude is considered to be small (of order less than unity) and low frequencies of modulation are considered. The coefficient of the linear term of the algebraic part of the Ginzburg–Landau equations is shown to exclusively hold the information on the amplitude and the frequency of modulation. The influence of nanoparticles (nanotubes) on heat transport in the presence/absence of various modulations is explained. The study reveals that the frequency of modulation is a dominant factor in the case of gravity and rotational modulations whereas in the case of boundary temperature modulation in addition to the frequency of modulation, the phase difference plays an important role. Effect of these three modulations is to enhance/diminish heat transport but depends strongly on the choice of values of frequency of modulation and amplitude. For fixed values of frequency ($\omega^* = 5$) and amplitude ($\delta_2 = 0.1$) of various modulations, it is shown that the maximum percentage of heat transport enhancement achieved in glycerin due to 5% of SWCNTs is 21.86% for gravity modulation, 17.36% for rotational modulation and 15.63% for boundary temperature modulation (out of phase). The reason for highest heat transport in gravity modulation is explained by finding area under the curves of three modulations. The study reveals that the modulation whose area under the curve is maximum transports maximum heat. The results pertaining to the single-phase model are recovered as a limiting case of the present study. The study shows that the single-phase model under-predicts heat transport compared to the two-phase model. The results obtained in the present study are compared with those of previous investigations and qualitatively good agreement is found.

Keywords Gravity · Boundary temperature · Rotation · Modulation · Nanoparticles · Nanotubes · Nanoliquid · Rayleigh–Bénard convection · Two-phase model · Lorenz model · Ginzburg–Landau equation

✉ P. G. Siddheshwar
mathdrpgs@gmail.com

C. Kanchana
kanchana@hit.edu.cn

Yi Zhao
zhao.yi@hit.edu.cn

¹ College of Science, Harbin Institute of Technology (Shenzhen), Nanshan District, Shenzhen 518055, Guangdong Province, China

² Department of Mathematics, Jnana Bharathi Campus, Bangalore University, Bengaluru 560056, India

Introduction

Rayleigh–Bénard convection (RBC) is a well-known convective phenomenon that occurs in nature and it has applications in many fields including the heat exchangers. In RBC, the following external mechanisms are considered as regulating mechanisms of heat transport:

1. Gravity modulation.
2. Boundary temperature modulation.
3. Rotational modulation.

Gravity modulation is essentially g-jitter or time-periodic body force, i.e., gravity-aligned oscillation of the Rayleigh–Bénard system. Modulated gravitational field effect on RBC has been of interest since long. Low-amplitude perturbation caused by crew motions, solar drag and other sources are experienced in a space-based experiment. The study on effect of gravitation modulation is of primary importance in such an experiment. It was Gershuni and Zhukhovitskii [1] who first reported the influence of g-jitter in an infinite extent horizontal plane confined with a Newtonian liquid. Gresho and Sani [2] investigated the effect of gravity modulation on a simple pendulum and reported a useful mechanical analogy. The effect of modulations of vertical temperature gradient and gravitational field on onset of convection using both physically realistic boundaries and free boundaries was studied by Gresho et al. [3]. An excellent review on gravity modulation was reported by Davis [4]. Biringen and Peltier [5] studied numerically the effect of sinusoidal and random modulations in different liquids by varying Prandtl number, and they concluded that compared to random modulation, sinusoidal modulation has effective stabilizing property in the three-dimensional RBC. Using high-frequency gravity modulation, Wheeler et al. [6] performed a linear stability analysis of RBC and reported the primary importance of frequency of modulation. Recently, Siddheshwar and Kanchana [7] and Siddheshwar and Meenakshi [8] studied the influence of three different wave-types of gravity-aligned oscillations (triangle, square and trigonometric sine) and showed that the influence of all the three types of wave-forms is to stabilize the Rayleigh–Bénard system in the presence/absence of nanoparticles and compared to the triangle wave-form, trigonometric sine wave-form transports maximum heat.

Venezian [9] made a linear stability analysis of the temperature-modulated RBC. Venezian [9] considered small amplitudes of modulation and obtained the shift in the critical Rayleigh number as a function of the driving frequency. Modulation of thermal instability at low frequency was investigated by Rosenblat and Herbert [10]. A classical Bénard problem with both steady and time-periodic components of modulation was considered by Rosenblat and Tanaka [11] in order to study the linear stability of the problem. Experimental and theoretical works on RBC under periodic external modulation was done by Ahlers et al. [12]. Schmitt and Lucke [13] derived an amplitude equation for convective rolls when the temperatures of the horizontal boundaries are modulated sinusoidally in time. Siddheshwar et al. [14] showed that the effect of temperature modulation on heat transfer depends not only on the frequency of temperature modulation but also on the phase difference. The combined effect of temperature modulation and rotation on RBC was investigated by Singh and Singh [15] using the classical Floquet theory. They studied harmonic and subharmonic

natures of instability depending upon the Coriolis force, frequency and amplitude.

The effect of rotation on onset of RBC was initiated by Chandrasekhar [16]. He showed that the disturbances in the liquid layer due to rotation results in a delay of the onset of convection. Bhattacharjee [17] showed that the threshold of convection can be raised or lowered depending on the Prandtl number and rotation speed. Küppers and Lortz [18] considered high rotation rates because of which the stable steady-state convective flow makes a direct transition to a weakly turbulent state. A number of laboratory studies confirmed that the onset of convection is indeed time-dependent [19, 20] although the mechanism for time dependence is different. Recently, Geurts and Kunnen [21] and Kooij et al. [22] studied heat transfer in a Rayleigh–Bénard configuration consisting of a vertical cylinder which is rotating about one of its axis and the rotation rate is modulated harmonically in time. For particular rotation rate, they observed an enhancement in heat transport.

Another innovative way of enhancing the heat transfer in RBC is using nanoliquid (Newtonian liquid suspended with dilute concentration of 10–100 nm sized metal/non-metal particles or carbon nanotubes) as a working medium. The keyword, *nanoliquid*, is introduced by Choi [23] who showed that there is a tremendous enhancement in thermal conductivity of baseliquid due to nanoparticles suspension. Thereafter, so many nanoliquid-related investigations were appeared in the literature using different nanomaterials and base liquids. A review on this aspect is provided by Azmi et al. [24] and Pinto and Firrelli [25]. Quite recently, Esfahani and Feshalami [26] made an interesting study on onset and heat transport in RBC in different nanoliquids using new empirical models. After peer review of the literature, it becomes apparent that compared to the study on modulation-imposed RBC in Newtonian liquids the study on modulation-imposed RBC in Newtonian nanoliquids is sparse. Yadav et al. [27] studied thermal instability of rotating nanofluids using the Galerkin method. The analytical expression of the critical Rayleigh number for both non-oscillatory and oscillatory cases was discussed. Bhadauria and Agarwal [28] studied the effect of rotation in a linear stability analysis of convection involving a Newtonian nanoliquid and explained the effect of various parameters on the critical Rayleigh number. Even though Yadav et al. [27] and Bhadauria and Agarwal [28] studied RBC in a Newtonian nanoliquid, they used base liquid properties in their study. The present study deviates from the study on RBC in nanoliquids reported by these investigators in the sense that the thermophysical properties of nanoliquids are included in the two-phase model. The two-phase model used in the present paper is proposed by Siddheshwar et al. [29] for the case of non-modulated system and used by many investigators [30–35]. Siddheshwar et al. [29] in their paper called

this model as *the generalized Buongiorno two-phase model*. We retain this name for the model in the current study also.

In some applications, for instance in the thermoacoustic engine [36] there is a need to regulate convection and have either a standing wave or traveling wave. Suppression of convection may be achieved by imposing suitable acoustics (modulation of acceleration or by vibration). Similarly in pulse tube cryocoolers, the convection is suppressed by acoustic. Thus, gravity modulation or vibration plays an important role in such devices to stabilize thermal convection. Rotational modulated RBC is an non-isothermal system that can throw light on a mixing process. An additional advantage in such mixing processes can be had by usage of nanoparticles/nanotubes of high thermal conductivity that might help in adding more vigor to a mixing process and might also help in the visualization of such a process. These above applications motivate the present study. The present study includes three different ways of modulating Rayleigh–Bénard convective system externally with same amplitude and frequency. The three different modulations considered in the paper are: gravity, boundary temperature and rotational modulations. Though the amplitude and the frequency of all the three modulations are assumed to be same, the outcome of these modulations is not similar, and this is because the gravity modulation and rotational modulation affect the momentum equation whereas the boundary temperature modulations affect the heat equation and the former modulations retain symmetry of the conduction state but the latter one induces a nonlinear conduction profile [37]. Due to these variations in modulations, there will be shift in the threshold of onset of convection and change in the Nusselt number value. An added advantage in heat transfer or in flow visualization can be had by the addition of nanoparticles/nanotubes in the base liquid. Thus, the present study throws light on many application situations. Five nanoparticles, two nanotubes and four base liquids are considered in the paper to obtain a combination of twenty-eight nanoliquids. The feasibility of using these nanoparticles/nanotubes are also discussed in the paper. The generalized Buongiorno two-phase model is used for the description of the nanoliquids. Using a truncated Fourier series representation, the generalized Lorenz model is obtained for each modulation problem. The Lorenz model is then transformed to the respective Ginzburg–Landau model using the method of multiscales [38]. The solution of the Ginzburg–Landau model is used in quantifying the heat transport in terms of the Nusselt number. With this background of the literature and mention on importance of the problem, we now move on to the formulation of the RBC problem in the presence of different types of modulations and in the presence/absence of nanoparticles.

Mathematical formulation

Description of the Rayleigh–Bénard convection setup

Let us consider an infinite extent horizontal nanoliquid layer between two thin parallel plates, $z = 0$ and $z = h$. The upper and lower plates are maintained at constant temperatures T_0 and $T_0 + \Delta T$ ($\Delta T > 0$). Further, since the working medium is considered to be a nanoliquid and two-phase model is adopted in the study we assume the upper and lower plates are maintained at constant nanoparticle concentrations ϕ_0 and $\phi_0 + \Delta\phi$ ($\Delta\phi > 0$), respectively. The system is subject to stress-free, isothermal and isonanoparticle concentration boundary conditions. The schematic of the setup is provided in Fig. 1.

Governing equations for nanoliquids

The governing system of equations in dimensional form for studying two-dimensional Rayleigh–Bénard convection (independent of the horizontal co-ordinate, y) in nanoliquids using the generalized Buongiorno two-phase model with the assumption of the Oberbeck–Boussinesq approximation and the small-scale convective motion are:

$$\nabla \cdot \mathbf{q} = 0, \quad (1)$$

$$\rho_{nl} \frac{\partial \mathbf{q}}{\partial t} = -\nabla p + \mu_{nl} \nabla^2 \mathbf{q} + [\rho_{nl} - (\rho\beta_1)_{nl}(T - T_0) + (\rho\beta_2)_{nl}(\phi - \phi_0)] \mathbf{g}, \quad (2)$$

$$(\rho C_p)_{nl} \left[\frac{\partial T}{\partial t} + (\mathbf{q} \cdot \nabla) T \right] = k_{nl} \nabla^2 T, \quad (3)$$

$$\frac{\partial \phi}{\partial t} + (\mathbf{q} \cdot \nabla) \phi = D_B \nabla^2 \phi + \frac{D_{Th}}{T_0} \nabla^2 T, \quad (4)$$

where $\mathbf{q} = (u, w)$ is the velocity vector in m, t is time in s, p is the pressure in Pa, $\mathbf{g} = (0, 0, -g)$, acceleration due to gravity in m s^{-2} , T is the temperature in K, ϕ is the normalized

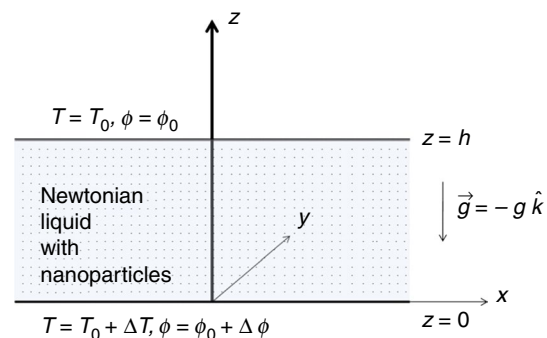


Fig. 1 Schematic of Rayleigh–Bénard convection problem

Table 1 Thermophysical properties of nanoliquids using phenomenological laws and mixture theory

Properties	Expression	Model
Effective viscosity	$\frac{\mu_{nl}}{\mu_{bl}} = \frac{1}{(1-\chi)^{2.5}}$	Brinkman model [39]
Effective thermal conductivity	$\frac{k_{nl}}{k_{bl}} = \frac{\left(\frac{k_{np}}{k_{bl}}\right)^{+(n-1)} - (n-1)\chi \left(1 - \frac{k_{np}}{k_{bl}}\right)}{\left(\frac{k_{np}}{k_{bl}}\right)^{+(n-1)} + \chi \left(1 - \frac{k_{np}}{k_{bl}}\right)}$	Hamilton–Crosser model [40]
Effective density	$\frac{\rho_{nl}}{\rho_{bl}} = (1-\chi) + \chi \frac{\rho_{np}}{\rho_{bl}}$	Mixture theory
Specific heat	$(C_p)_{nl} = \frac{(\rho C_p)_{nl}}{\rho_{nl}}$ where $(\rho C_p)_{nl} = (\rho C_p)_{bl}(1-\chi) + \chi(\rho C_p)_{np}$	Mixture theory
Thermal and nanoparticle concentration expansion coefficients	$\beta_{inl} = \frac{(\rho\beta_i)_{nl}}{\rho_{nl}}$ $(\rho\beta_i)_{nl} = (\rho\beta_i)_{bl}(1-\chi) + \chi(\rho C_p)_{np}$	Hamilton–Crosser model [40] and mixture theory
Thermal diffusivity	$\alpha_{nl} = \frac{k_{nl}}{(C_p)_{nl}}$	Hamilton–Crosser model [40] and mixture theory

nanoparticles/nanotube volume fraction, μ_{nl} , ρ_{nl} , β_{1nl} , β_{2nl} , C_{pnl} and k_{nl} , respectively represent dynamic viscosity (in kg ms^{-1}), density (in kg m^{-2}), thermal expansion coefficient (in K^{-1}), nanoparticles/nanotube expansion coefficient (in kg^{-1}), specific heat (in $\text{J kg}^{-1} \text{K}^{-1}$) and thermal conductivity (in $\text{W m}^{-1} \text{K}^{-1}$) of nanoliquid and are calculated using either phenomenological laws or mixture theory (see Table 1).

The term, n , in Hamilton–Crosser model represents the shape factor for spherical shaped nanoparticles, $n = 3$ for nanotubes $n = 3.75$.

The term, D_B and D_{Th} represent the diffusion coefficients and are defined as:

$$D_B = \frac{K_B T}{3\pi\mu_{nl}d_h} \text{ and } D_{Th} = 0.26 \frac{k_{nl}}{2k_{nl} + k_{np}} \frac{\mu_{nl}}{\rho_{nl}} \chi \quad (5)$$

where d_h denotes hydrodynamic diameter. In the paper, we considered both spherical-shaped nanoparticles and nanotubes. For nanoparticles $d_h = d_{np}$, average diameter of nanoparticles and in the case of nanotubes,

$$d_h = \frac{l}{\log\left(\frac{l}{d_{nt}}\right) + 0.32}, \quad (6)$$

where d_{nt} denotes the nanotube diameter and l is the length of nanotubes.

The governing system of Eqs. (1)–(4) is subject to stress-free, isothermal and iso-nanoparticles' concentration boundary condition:

$$\left. \begin{aligned} u = 0, w = 0, S_{xz} = 0, T = T_0 + \Delta T, \phi = \phi_0 + \Delta\phi \text{ at } z = 0 \\ u = 0, w = 0, S_{xz} = 0, T = T_0, \phi = \phi_0 \text{ at } z = h \end{aligned} \right\} \quad (7)$$

where u and w are the i th and k th-components of velocity vector, \mathbf{q} and $S_{xz} = \mu_{nl} \left(\frac{\partial u}{\partial z} + \frac{\partial w}{\partial x} \right)$.

We now impose time-periodic external driving forces to the aforementioned hydrodynamical system to study the influence of various parameters on heat transport. We first study the effect of time-periodic gravity-aligned oscillations on Rayleigh–Bénard convection in Newtonian liquids as well as Newtonian nanoliquids.

Gravity modulation

Modulation of gravitational force is achieved by periodically oscillating the nanoliquid layer vertically with time, t (see Fig. 2). Thus, the gravitational acceleration in the equation of linear momentum (2) now takes the form:

$$\mathbf{g} = (0, 0, -[g + g'(\omega, t)]), \quad (8)$$

where ω is frequency of modulation.

In the quiescent basic state, we have

$$\mathbf{q} = 0, p = p_b(z), T = T_b(z), \phi = \phi_b(z), \quad (9)$$

Using Eq. (9) in the governing Eqs. (1)–(4) and substituting boundary condition (7), we get the temperature and the nanoparticles' distribution determined by conduction and are given below:

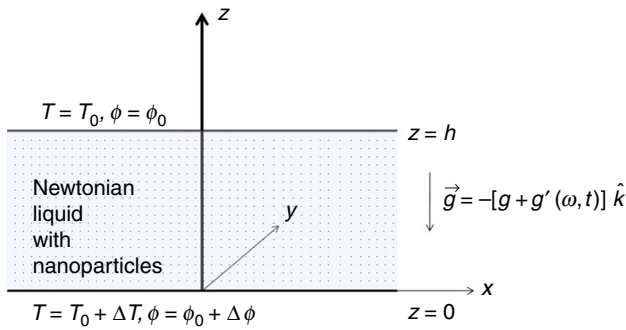


Fig. 2 Schematic of the gravity-modulated Rayleigh–Bénard convection problem

$$\left. \begin{aligned} T_b(z) &= \left(1 - \frac{z}{h}\right) \Delta T + T_0, \\ \phi_b(z) &= \left(1 - \frac{z}{h}\right) \Delta \phi + \phi_0 \end{aligned} \right\} \quad (10)$$

We apply the following perturbations (due to an external heating and the vertical vibration) on the basic state solution:

$$\left. \begin{aligned} \mathbf{q} &= \mathbf{q}'(x, z, t), \quad p = p_b(z) + p'(x, z, t), \\ T &= T_b(z) + T'(x, z, t), \quad \phi = \phi_b(z) + \phi'(x, z, t) \end{aligned} \right\}, \quad (11)$$

where T_b and ϕ_b are obtained from Eq. (10).

Using the perturbations (11) in Eqs. (2)–(4), we get the governing equation in perturbed form. We eliminate the pressure term in the resulting equations and we introduce the following stream function, ψ :

$$u = -\frac{\partial \psi}{\partial z}, \quad w = \frac{\partial \psi}{\partial x}, \quad (12)$$

that yields the following system of partial differential equations:

$$\begin{aligned} \rho_{nl} \frac{\partial}{\partial t} (\nabla^2 \psi) &= \mu_{nl} \nabla^2 \psi + [g + g'(\omega, t)] \\ &\times \left((\rho \beta_1)_{nl} \frac{\partial T'}{\partial x} - (\rho \beta_2)_{nl} \frac{\partial \phi'}{\partial x} \right), \end{aligned} \quad (13)$$

$$\begin{aligned} (\rho C_p)_{nl} \left[\frac{\partial T'}{\partial t} + \frac{\partial \psi}{\partial x} \frac{\partial T'}{\partial z} - \frac{\partial \psi}{\partial z} \frac{\partial T'}{\partial x} + \frac{\partial \psi}{\partial x} \frac{dT_b}{dz} \right] \\ = k_{nl} \nabla^2 T', \end{aligned} \quad (14)$$

$$\begin{aligned} \frac{\partial \phi'}{\partial t} + \frac{\partial \psi}{\partial x} \frac{\partial \phi'}{\partial z} - \frac{\partial \psi}{\partial z} \frac{\partial \phi'}{\partial x} - \frac{\partial \psi}{\partial x} \frac{d\phi_b}{dz} \\ = D_B \nabla^2 \phi' + \frac{D_{Th}}{T_0} \nabla^2 T'. \end{aligned} \quad (15)$$

Introducing the following nondimensional variables

$$(X, Z) = \left(\frac{x}{h}, \frac{z}{h} \right), \quad \tau = \frac{\alpha_{bl} t}{h^2}, \quad \Psi = \frac{\psi}{\alpha_{bl}}, \quad (16)$$

$$\Theta = \frac{T'}{\Delta T}, \quad \Phi = \frac{\phi'}{\Delta \phi},$$

into Eqs. (13)–(15), we get the governing equations in non-dimensional form as:

$$\begin{aligned} \frac{1}{Pr_{nl}} \frac{\partial}{\partial \tau} (\nabla^2 \Psi) &= a_1 \nabla^4 \Psi + [1 + g_m(\omega, \tau)] Ra_{nl} a_1^2 \frac{\partial \Theta}{\partial X} \\ &- [1 + g_m(\omega, \tau)] Ra_{\phi_{nl}} a_1^2 \frac{\partial \Phi}{\partial X} \end{aligned} \quad (17)$$

$$\frac{\partial \Theta}{\partial \tau} = a_1 \nabla^2 \Theta + \frac{\partial \Psi}{\partial X} - J(\Psi, \Theta), \quad (18)$$

$$\frac{\partial \Phi}{\partial \tau} = \frac{a_1}{Le_{nl}} \nabla^2 \Phi + \frac{a_1 N_{A_{nl}}}{Le_{nl}} \nabla^2 \Theta + \frac{\partial \Psi}{\partial X} - J(\Psi, \Phi), \quad (19)$$

where $Pr_{nl} = \frac{\mu_{nl}}{\rho_{nl} \alpha_{nl}}$ is the nanoliquid Prandtl number, $a_1 = \frac{\alpha_{nl}}{\alpha_{bl}}$ is the diffusivity ratio, $Ra_{nl} = \frac{(\rho \beta_1)_{nl} \Delta T h^3 g}{\mu_{nl} \alpha_{nl}}$ is the

thermal Rayleigh number, $Ra_{\phi_{nl}} = \frac{(\rho_{np} - \rho_{nl}) \Delta \Phi h^3 g}{\mu_{nl} \alpha_{nl}}$ is the concentration Rayleigh number, $Le_{nl} = \frac{\alpha_{nl}}{D_B \Delta \Phi}$ is the Lewis

number, $N_{A_{nl}} = \frac{D_{Th} \Delta T}{D_B T_0 \Delta \Phi}$ is the modified diffusivity ratio.

In Eqs. (18) and (19), $J(\Psi, \Theta)$ and $J(\Psi, \Phi)$ are Jacobians defined as $J(\Psi, \Theta) = \frac{\partial \Psi}{\partial X} \frac{\partial \Theta}{\partial Z} - \frac{\partial \Psi}{\partial Z} \frac{\partial \Theta}{\partial X}$ and $J(\Psi, \Phi) = \frac{\partial \Psi}{\partial X} \frac{\partial \Phi}{\partial Z} - \frac{\partial \Psi}{\partial Z} \frac{\partial \Phi}{\partial X}$ and in Eq. (17),

$g_m(\omega, \tau) = \frac{g}{g'(\omega, \tau)}$ arises due to gravity modulation.

It is clear from the definition of nondimensional parameter that the governing Eqs. (17)–(19) involve the thermo-physical properties of nanoliquids which deviates the present study with the classical Buongiorno model [41].

The boundary condition (7) in nondimensional form written as:

$$\Psi = \frac{\partial^2}{\partial Z^2} \left(\frac{\partial \Psi}{\partial X} \right) = \Theta = \Phi = 0 \text{ at } Z = 0, 1. \quad (20)$$

By previous instigation [32], it is now well-known that the minimal mode truncated Fourier series representation is good enough to approximate solution. Hence using a minimal truncated representation we perform a weakly nonlinear stability analysis in the next subsection.

Weakly nonlinear stability analysis

We assume the solution to the stream function, temperature and nanoparticles’ concentration as the following minimal mode truncation form:

$$\Psi = \frac{\sqrt{2}a_1\delta^2}{\pi^2\kappa_c} \mathcal{A}(\tau) \sin(\pi\kappa_c X) \sin(\pi Z), \tag{21}$$

$$\Theta = \frac{\sqrt{2}}{\pi r_{nl}} \mathcal{B}(\tau) \cos(\pi\kappa_c X) \sin(\pi Z) - \frac{1}{\pi r_{nl}} \mathcal{C}(\tau) \sin(2\pi Z), \tag{22}$$

$$\Phi = \frac{\sqrt{2}}{\pi} \mathcal{L}(\tau) \cos(\pi\kappa_c X) \sin(\pi Z) + \frac{1}{\pi} \mathcal{M}(\tau) \sin(2\pi Z), \tag{23}$$

where $r_{nl} = \frac{Ra_{nl}\pi^2\kappa_c^2}{\delta^6}$, κ_c is the critical wave number and $\delta^2 = \pi^2(1 + \kappa_c^2)$. The coefficient of amplitudes, $\mathcal{A}, \mathcal{B}, \mathcal{C}, \mathcal{L}$ and \mathcal{M} represent the scaling. With these scalings, we get the generalized Lorenz model which resembles the classical Lorenz model in the limiting case (in the absence of modulation and nanoparticles).

Substituting the solution (21)–(23) into the governing Eqs. (17)–(19) and using orthogonality condition with the corresponding eigenfunctions $\sin(\pi\kappa_c X) \sin(\pi Z)$, $\cos(\pi\kappa_c X) \sin(\pi Z)$ and $\sin(2\pi Z)$, we get the following generalized Lorenz system which involves the properties of nanoparticles and base liquid and the influence of the gravity-aligned oscillation:

$$\frac{1}{Pr_{nl}} \frac{d\mathcal{A}}{d\tau_1} = a_1(-\mathcal{A} + [1 + g_m(\omega, \tau_1)]\mathcal{B} - [1 + g_m(\omega, \tau_1)]r_{\phi_{nl}}\mathcal{L}), \tag{24}$$

$$\frac{d\mathcal{B}}{d\tau_1} = a_1(r_{nl}\mathcal{A} - \mathcal{B} - \mathcal{A}\mathcal{C}), \tag{25}$$

$$\frac{d\mathcal{C}}{d\tau_1} = a_1(\mathcal{A}\mathcal{B} - b_1\mathcal{C}), \tag{26}$$

$$r_{nl} \frac{d\mathcal{L}}{d\tau_1} = a_1 \left(r_{nl}\mathcal{A} - \frac{N_{A_{nl}}}{Le_{nl}}\mathcal{B} - \frac{r_{nl}}{Le_{nl}}\mathcal{L} + r_{nl}\mathcal{A}\mathcal{M} \right), \tag{27}$$

$$r_{nl} \frac{d\mathcal{M}}{d\tau_1} = a_1 \left(\frac{b_1 N_{A_{nl}}}{Le_{nl}}\mathcal{C} - \frac{b_1 r_{nl}}{Le_{nl}}\mathcal{M} - r_{nl}\mathcal{A}\mathcal{L} \right), \tag{28}$$

where $\tau_1 = \delta^2\tau$, $r_{\phi_{nl}} = \frac{Ra_{\phi_{nl}}\pi^2\kappa_c^2}{\delta^6}$ and $b_1 = \frac{4\pi^2}{\delta^2}$.

In the paper, the gravity modulation is taken to be a trigonometric sine function, viz., $g_m(\omega, \tau_1) = \epsilon^2\delta_2 \sin(\omega\tau_1)$. The factor ϵ^2 is included with the amplitude, δ_2 , to emphasize that the modulation considered in the paper to be of small amplitude that facilitates the use of a regular perturbation expansion in Eqs. (24)–(28) in terms of ϵ :

$$\begin{bmatrix} \mathcal{A} \\ \mathcal{B} \\ \mathcal{C} \\ \mathcal{L} \\ \mathcal{M} \\ r_{nl} \end{bmatrix} = \begin{bmatrix} 0 \\ 0 \\ 0 \\ 0 \\ 0 \\ 1 \end{bmatrix} + \epsilon \begin{bmatrix} A_1 \\ B_1 \\ C_1 \\ L_1 \\ M_1 \\ 0 \end{bmatrix} + \epsilon^2 \begin{bmatrix} A_2 \\ B_2 \\ C_2 \\ L_2 \\ M_2 \\ r_2 \end{bmatrix} + \epsilon^3 \begin{bmatrix} A_3 \\ B_3 \\ C_3 \\ L_3 \\ M_3 \\ 0 \end{bmatrix} + \dots \tag{29}$$

We assume the time variations only at the small scale $\tau_1^* = \epsilon^2\tau_1$ and hence $g_m(\omega^*, \tau_1^*) = \epsilon^2\delta_2 \sin(\omega^*\tau_1^*)$ where $\omega^* = \frac{\omega}{\epsilon^2}$. The nondimensional parameter, $N_{A_{nl}}$, describes the thermophoretic effect and is assumed to be weak and arises in the order of ϵ^2 . For the sake of mathematical convenience, we define the operators

$$L = \begin{bmatrix} -a_1 & a_1 & 0 & -a_1 r_{\phi_{nl}} & 0 \\ a_1 & a_1 & 0 & 0 & 0 \\ 0 & 0 & -b_1 a_1 & 0 & 0 \\ a_1 & 0 & 0 & -\frac{a_1}{Le_{nl}} & 0 \\ 0 & 0 & 0 & 0 & -\frac{a_1 b_1}{Le_{nl}} \end{bmatrix} \text{ and } U_i = \begin{bmatrix} A_i \\ B_i \\ C_i \\ L_i \\ M_i \end{bmatrix}, \quad i = 1(1)3. \tag{30}$$

On applying regular perturbation Eq. (29) into the governing system of Eqs. (24)–(28) and extracting $o(\epsilon)$, $o(\epsilon^2)$ and $o(\epsilon^3)$ on either side of the resulting equations, we get system of homogeneous/nonhomogeneous equations.

At $o(\epsilon)$, we get a homogeneous system:

$$LU_1 = 0, \tag{31}$$

Solving the above system, we get the following solution

$$[A_1, B_1, C_1, L_1, M_1]^{Tr} = [A_{1_0}, \mathcal{A}_{1_0}, 0, Le_{nl}\mathcal{A}_{1_0}, 0]^{Tr}, \tag{32}$$

where \mathcal{A}_{1_0} is an arbitrary function of τ_1^* . At $o(\epsilon^2)$, we get a nonhomogeneous system:

$$LU_2 = [R_{21}, R_{22}, R_{23}, R_{24}, R_{25}]^{Tr}, \tag{33}$$

where

$$\begin{aligned} R_{21} &= 0, R_{22} = a_1A_1C_1, R_{23} = -a_1A_1B_1, \\ R_{24} &= -A_1M_1, R_{25} = -A_1L_1. \end{aligned} \tag{34}$$

Substituting the solution of first-order system, i.e., Eq. (32), in the (33) and solving the resultant equations, we get solution of second-order system:

$$[A_2, B_2, C_2, L_2, M_2]^{Tr} = \left[0, 0, \frac{1}{b_1}\mathcal{A}_{1_0}^2, 0, \frac{-Le_{nl}^2}{b_1}\mathcal{A}_{1_0}^2 \right]^{Tr}, \tag{35}$$

At $o(\epsilon^3)$, we get a nonhomogeneous system:

$$LU_3 = [R_{31}, R_{32}, R_{33}, R_{34}, R_{35}]^{Tr}, \tag{36}$$

where

$$\left. \begin{aligned} R_{31} &= \frac{1}{Pr_{nl}} \frac{dA_1}{d\tau_1^*} - a_1Pr_{nl}\delta_2 \sin(\omega^*\tau_1^*)B_1 + a_1Pr_{nl}r_{\phi_{nl}}\delta_2 \sin(\omega^*\tau_1^*)L_1, \\ R_{32} &= \frac{dB_1}{d\tau_1^*} - a_1r_2A_1 + a_1A_1C_2, \\ R_{33} &= -a_1(A_1B_2 + A_2B_1) + \frac{dC_1}{d\tau_1^*}, \\ R_{34} &= -a_1(A_1M_2 + A_2M_1) + \frac{dL_1}{d\tau_1^*} - a_1r_2A_1 + a_1\frac{N_{A_{nl}}}{Le_{nl}}B_1 + \frac{1}{Le_{nl}}L_1, \\ R_{35} &= a_1(A_1L_2 + A_2L_1) + \frac{dM_1}{d\tau_1^*} + \frac{a_1b_1r_2}{Lev}M_1. \end{aligned} \right\} \tag{37}$$

At the third-order system, we determine the amplitude, \mathcal{A}_{1_0} , using the Fredholm solvability condition which states that ‘the inhomogeneous terms must be orthogonal to the solution of the homogenous system’, i.e.,

$$R_{31}\hat{A}_1 + R_{32}\hat{B}_1 + R_{33}\hat{C}_1 + R_{34}\hat{L}_1 + R_{35}\hat{M}_1 = 0, \tag{38}$$

where $(\hat{A}_1, \hat{B}_1, \hat{C}_1, \hat{L}_1, \hat{M}_1)$ denote the solution of adjoint system (31).

Equation (38) yields to the Ginzburg–Landau equation:

$$\frac{d\mathcal{A}_{1_0}(\tau_1^*)}{d\tau_1^*} = Q_1\mathcal{A}_{1_0}(\tau_1^*) - Q_2\mathcal{A}_{1_0}^3(\tau_1^*). \tag{39}$$

The expressions for the coefficients Q_1 and Q_2 are, respectively, given by:

$$\left. \begin{aligned} Q_1 &= \frac{a_1Pr_{nl}[r_2 + N_{A_{nl}}r_{\phi_{nl}} + \delta_2 \sin(\omega^*\tau_1^*)(r_0 - r_{\phi_{nl}}Le_{nl})]}{1 + Pr_{nl}(r_0 - Le_{nl}^2r_{\phi_{nl}})}, \\ Q_2 &= \frac{Pr_{nl}(r_0 - Le_{nl}^3r_{\phi_{nl}})}{b_1[1 + Pr_{nl}(r_0 - Le_{nl}^2r_{\phi_{nl}})]}. \end{aligned} \right\} \tag{40}$$

On taking $r_{\phi_{nl}} = 0$ in Eq. (39), we arrive at the Ginzburg–Landau equation for Newtonian liquids reported by Siddheshwar [42].

We next study the influence of boundary temperature modulation on Rayleigh–Bénard convection in Newtonian liquids and Newtonian nanoliquids.

Boundary temperature modulation

The boundary temperature modulation in Rayleigh–Bénard convection is achieved by imposing externally a time-periodic boundary temperature with small amplitude, $\epsilon^2\delta_2$, phase difference, φ , and frequency, ω . In the problem of the generalized Buongiorno two-phase model, it is necessary to consider the wall introduction of nanoparticles’ concentration in addition to wall temperature. The schematic of the problem is shown in Fig. 3. The governing system of equations in dimensional form for studying Rayleigh–Bénard convection in nanoliquids using a two-phase model are Eqs. (1)–(4).

The external imposed wall temperatures (Venezian [9]) are

$$\left. \begin{aligned} T &= T_0 + \frac{\Delta T}{2} [1 + \epsilon^2\delta_2 \cos(\omega t)] \quad \text{at } z = 0, \\ T &= T_0 - \frac{\Delta T}{2} [1 - \epsilon^2\delta_2 \cos(\omega t + \varphi)] \quad \text{at } z = h, \end{aligned} \right\} \tag{41}$$

Similarly, for wall introduction of concentration we need to take:

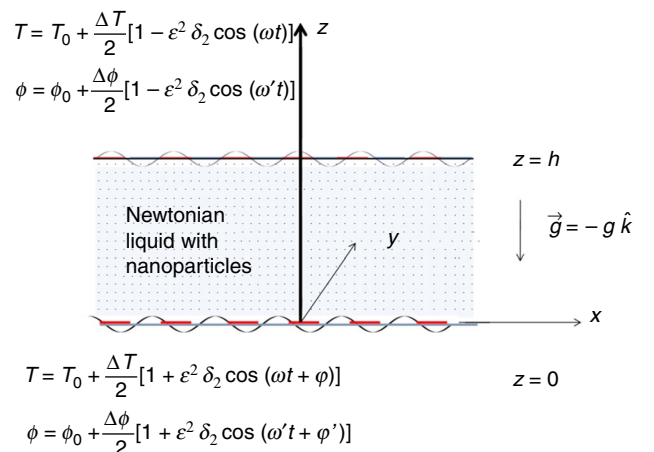


Fig. 3 Schematic of Rayleigh–Bénard convection with boundary temperature modulation

$$\left. \begin{aligned} \phi &= \phi_0 + \frac{\Delta\phi}{2} [1 + \epsilon^2 \delta_2 \cos(\omega t)] \quad \text{at } z = 0, \\ \phi &= \phi_0 - \frac{\Delta\phi}{2} [1 - \epsilon^2 \delta_2 \cos(\omega t + \varphi)] \quad \text{at } z = h, \end{aligned} \right\} \quad (42)$$

The velocity, pressure, temperature and nanoparticles' concentration fields in the quiescent basic state are given by

$$q_b(z) = (0, 0), \quad p = p_b(z, t), \quad T_b = T_b(z, t), \\ \phi_b = \phi_b(z, t),$$

which satisfy the following equations:

$$-\frac{dp_b}{dz} = [\rho_{nl} - (\rho\beta)_{nl}(T_b - T_0)]g, \quad (43)$$

$$\frac{\partial T_b}{\partial t} = \alpha_{nl} \frac{\partial^2 T_b}{\partial z^2}, \quad (44)$$

$$\frac{\partial \phi_b}{\partial t} = D_B \frac{\partial^2 \phi_b}{\partial z^2} + \frac{D_T}{T_0} \frac{\partial^2 T_b}{\partial z^2}. \quad (45)$$

Equations (44) and (45) consist of the sum of a steady part and an oscillating part:

$$T_b = T_s(z) + \epsilon^2 T_1(z, t), \quad (46)$$

$$\phi_b = \phi_s(z) + \epsilon^2 \phi_1(z, t). \quad (47)$$

Solving Eqs. (43)–(45) with the help of Eqs. (46) and (47) and using the boundary conditions (41) and (42), we get

$$T_b(z, t) = T_0 + \Delta T \left(\frac{1}{2} - \frac{z}{h} \right) + \epsilon^2 \delta_2 \text{Re} \{ [a(\lambda_1) e^{\lambda_1 z} + a(-\lambda) e^{-\lambda z}] e^{-i\omega t} \}, \quad (48)$$

$$\begin{aligned} \phi_b(z, t) &= \phi_0 + \Delta\phi \left(\frac{1}{2} - \frac{z}{h} \right) \\ &+ \epsilon^2 \delta_2 \text{Re} \{ [a(\lambda_1) e^{\lambda_1 z} + a(-\lambda_1) e^{-\lambda_1 z}] e^{-i\omega t} \} \\ &+ N_{A_{nl}} \left[\frac{\lambda^2}{\lambda^2 - \lambda_1^2} \left[\left(\frac{e^{\lambda_1 z} - e^{-\lambda_1 z}}{e^{\lambda_1 h} - e^{-\lambda_1 h}} \right) \right. \right. \\ &\quad \left. \left. (a'(\lambda, \lambda_1) + a'(-\lambda, -\lambda_1)) + a'(-\lambda, -\lambda_1) \right) \right. \\ &\quad \left. + a(\lambda)(e^{-\lambda_1 z} - e^{\lambda z}) \right. \\ &\quad \left. + a(-\lambda)(e^{-\lambda_1 z} - e^{\lambda z}) \right] \}, \end{aligned} \quad (49)$$

where

$$a'(\lambda, \lambda_1) = \frac{\Delta T}{2} \left[\frac{e^{-i\varphi} - e^{-\lambda h}}{e^{\lambda h} - e^{-\lambda h}} \right] (e^{\lambda h} - e^{\lambda_1 h}), \quad (50)$$

$$a(\lambda_1) = \frac{\Delta T}{2} \left[\frac{e^{-i\varphi} - e^{-\lambda h}}{e^{\lambda h} - e^{-\lambda h}} \right], \quad (51)$$

$$\lambda = (1 - i) \sqrt{\frac{\omega h^2}{2\alpha_{nl}}},$$

$$a(\lambda_1) = \frac{\Delta\phi}{2} \left[\frac{e^{-i\varphi} - e^{-\lambda_1 h}}{e^{\lambda_1 h} - e^{-\lambda_1 h}} \right], \quad (52)$$

$$\lambda_1 = (1 - i) \sqrt{\frac{\omega h^2}{2D_B}}.$$

Applying perturbations (11) on the basic state solution (48) and (49) and introducing the stream function (12) and the scaling (16), the governing equations take the form:

$$\frac{1}{Pr_{nl}} \frac{\partial}{\partial \tau} (\nabla^2 \Psi) = a_1 \nabla^4 \Psi + Ra_{nl} a_1^2 \frac{\partial \Theta}{\partial X} - Ra_{\phi_{nl}} a_1^2 \frac{\partial \Phi}{\partial X} \quad (53)$$

$$\frac{\partial \Theta}{\partial \tau} = a_1 \nabla^2 \Theta - J(\Psi, \Theta) - [\epsilon^2 \delta_2 f(Z, \tau) - 1] \frac{\partial \Psi}{\partial X}, \quad (54)$$

$$\begin{aligned} \frac{\partial \Phi}{\partial \tau} &= \frac{a_1}{Le_{nl}} \nabla^2 \Phi + \frac{a_1 N_{A_{nl}}}{Le_{nl}} \nabla^2 \Theta - J(\Psi, \Phi) \\ &- [\epsilon^2 \delta_2 [g(Z, \tau) + N_{A_{nl}} g_1(Z, \tau)] - 1] \frac{\partial \Psi}{\partial X}, \end{aligned} \quad (55)$$

where

$$f(Z, \tau) = \text{Re} \{ A(\lambda) e^{\lambda Z} + A(\lambda) e^{-\lambda Z} \} e^{-i\omega^* \tau}, \quad (56)$$

$$A(\lambda) = \frac{\lambda}{2} \left(\frac{e^{i\varphi} - e^{-\lambda}}{e^{\lambda} - e^{-\lambda}} \right), \quad \lambda = (1 - i) \sqrt{\frac{\omega^*}{2a_1}}, \quad (57)$$

$$g(Z, \tau) = \text{Re} \{ A_1(\lambda_1) e^{\lambda_1 Z} + A_1(-\lambda_1) e^{-\lambda_1 Z} \} e^{-i\omega^* \tau}, \quad (58)$$

$$A_1(\lambda_1) = \frac{\lambda_1}{2} \left(\frac{e^{i\varphi} - e^{-\lambda_1}}{e^{\lambda_1} - e^{-\lambda_1}} \right), \quad \lambda_1 = (1 - i) \sqrt{\frac{\omega^* Le_{nl}}{2a_1}}, \quad (59)$$

$$g_1(Z, \tau) \lambda_1 [M(\lambda_1, \lambda) + M(\lambda_1, -\lambda)] (e^{\lambda_1 Z} + e^{-\lambda_1 Z}) - N(\lambda_1, \lambda) (\lambda_1 e^{-\lambda_1 Z} + \lambda e^{\lambda Z}) + N(\lambda_1, -\lambda) (\lambda e^{\lambda Z} - \lambda_1 e^{-\lambda_1 Z}), \quad (60)$$

$$M(\lambda_1, \lambda) = \frac{\lambda_1}{2} \frac{1}{1 - \left(\frac{\lambda_1}{\lambda} \right)^2} \left(\frac{e^{-i\varphi} - e^{-\lambda_1}}{e^{\lambda_1} - e^{-\lambda_1}} \right) \left(\frac{e^{\lambda} - e^{-\lambda_1}}{e^{\lambda_1} - e^{-\lambda_1}} \right), \quad (61)$$

$$N(\lambda_1, \lambda) = \frac{1}{2 \left(1 - \left(\frac{\lambda_1}{\lambda} \right)^2 \right)} \left(\frac{e^{-i\varphi} - e^{-\lambda_1}}{e^{\lambda_1} - e^{-\lambda_1}} \right). \tag{62}$$

Weakly nonlinear stability analysis

Following the procedure of Sec. (2.3), we get the fifth-order Lorenz model for the boundary temperature-modulated convection problem in the form:

$$\frac{1}{Pr_{nl}} \frac{dA}{d\tau_1} = a_1 (B - A - r_{\phi_{nl}} C), \tag{63}$$

$$\frac{dB}{d\tau_1} = a_1 (r_{nl} A - B - AC - 2\epsilon^2 r_{nl} \delta_2 F(\tau) A), \tag{64}$$

$$\frac{dC}{d\tau_1} = a_1 (AB - bC), \tag{65}$$

$$r_{nl} \frac{d\mathcal{L}}{d\tau_1} = a_1 \left(r_{nl} A - \frac{N_{A_{nl}}}{Le_{nl}} B - \frac{r_{nl}}{Le_{nl}} \mathcal{L} + r_{nl} A \mathcal{M} + 2\epsilon^2 \delta^2 r_{nl} [G(\tau) + \epsilon^2 N_{A_{nl}} G_1(\tau)] A \right), \tag{66}$$

$$r_{nl} \frac{d\mathcal{M}}{d\tau_1} = a_1 \left(\frac{b_1 N_{A_{nl}}}{Le_{nl}} C - \frac{b_1 r_{nl}}{Le_{nl}} \mathcal{M} - r_{nl} A \mathcal{L} \right), \tag{67}$$

where

$$F(\tau) = \int_{X=0}^{\frac{2\pi}{\pi\kappa c}} \int_{Z=0}^1 f(Z, \tau) \cos^2(\pi\kappa X) \sin^2(\pi Z) dXdZ, \tag{68}$$

$$G(\tau) = \int_{X=0}^{\frac{2\pi}{\pi\kappa c}} \int_{Z=0}^1 g(Z, \tau) \cos^2(\pi\kappa X) \sin^2(\pi Z) dXdZ, \tag{69}$$

$$G_1(\tau) = \int_{X=0}^{\frac{2\pi}{\pi\kappa c}} \int_{Z=0}^1 g_1(Z, \tau) \cos^2(\pi\kappa X) \sin^2(\pi Z) dXdZ. \tag{70}$$

Using an identical procedure to that in subsection (2.3), the Ginzburg–Landau equation for the boundary temperature modulation problem may be obtained in the form:

$$\frac{dA_{1_0}(\tau_1^*)}{d\tau_1^*} = Q_3 A_{1_0}(\tau_1^*) - Q_4 A_{1_0}^3(\tau_1^*), \tag{71}$$

where

$$\left. \begin{aligned} Q_3 &= \frac{a_1 Pr_{nl} (r_2 + N_{A_{nl}} r_{\phi_{nl}} - 2\delta_2 [r_0 F(\tau) + r_{\phi_{nl}} Le_{nl} G(\tau)])}{1 + Pr_{nl} (r_0 - Le_{nl}^2 r_{\phi_{nl}})}, \\ Q_4 &= \frac{a_1 Pr_{nl} (r_0 - Le_{nl}^3 r_{\phi_{nl}})}{b_1 [1 + Pr_{nl} (r_0 - Le_{nl}^2 r_{\phi_{nl}})]}. \end{aligned} \right\} \tag{72}$$

Having obtained the Ginzburg–Landau equation of the gravity-modulated and boundary temperature-modulated convection problems, we next derive the time-dependent Ginzburg–Landau equation for Rayleigh–Bénard convection in Newtonian liquids and Newtonian nanoliquids in the presence of rotational modulation.

Rotational modulation

In the case of rotational modulation, the nanoliquid layer is assumed to be in rotation about the axis of z , with a constant angular velocity, Ω . The motion described here occurs as it in a way as it appears to an observer at rest in a frame rotating about the same axis and with the same angular velocity. The governing system of equations in dimensional form for studying two-dimensional Rayleigh–Bénard convection in nanoliquids are given in Eq. (1)–(4) with an additional term $2\rho_{nl_0}(\mathbf{q} \times \Omega)$ in the linear momentum Eq. (2). The term $(\mathbf{q} \times \Omega)$ represents the Coriolis acceleration (see Chandrasekhar [16]) with the time-periodic angular acceleration, $\Omega(t) = \Omega[1 + \epsilon^2 \delta_2 \cos(\omega t)]$ and $\epsilon^2 \delta_2$ is its amplitude and ω is frequency. Schematic of the same is shown in Fig. 4.

The basic state solution of the rotational modulation problem is given by Eq. (10). Superimposing the perturbation, (11), on the basic state solution and using the resultant equations in Eqs. (1)–(4), eliminating the pressure and introducing the stream function, we get the nondimensional form of the governing equations to study rotating Rayleigh–Bénard convection in nanoliquids in the following form:

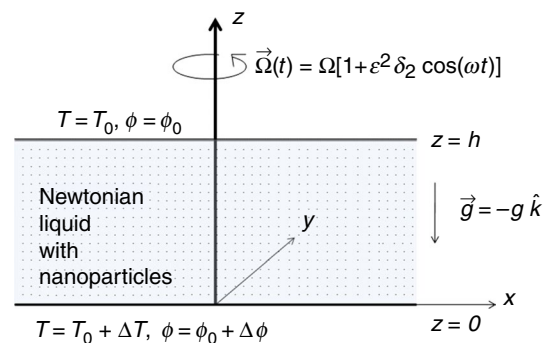


Fig. 4 Schematic of rotationally modulated Rayleigh–Bénard convection problem

$$\rho_{nl} \frac{\partial}{\partial t} (\nabla^2 \psi) = \mu_{nl} \nabla^2 \psi + 2\rho_{nl_0} \Omega [1 + \epsilon^2 \delta_2 \cos(\omega t)] \frac{\partial v}{\partial z} + (\rho\beta)_{nl} \frac{\partial T'}{\partial x} g - (\rho\beta)_\phi \frac{\partial \phi'}{\partial x} g, \tag{73}$$

$$\rho_{nl} \left[\frac{\partial v}{\partial t} + J(\psi, v) \right] = \mu_{nl} \nabla^2 v + 2\rho_{nl_0} \Omega [1 + \epsilon^2 \delta_2 \cos(\omega t)] \frac{\partial \psi}{\partial z}, \tag{74}$$

$$(\rho C_p)_{nl} \left[\frac{\partial T'}{\partial t} + \frac{\partial \psi}{\partial x} \frac{\partial T'}{\partial z} - \frac{\partial \psi}{\partial z} \frac{\partial T'}{\partial x} + \frac{\partial \psi}{\partial x} \frac{dT_b}{dz} \right] = k_{nl} \nabla^2 T', \tag{75}$$

$$\frac{\partial \phi'}{\partial t} + \frac{\partial \psi}{\partial x} \frac{\partial \phi'}{\partial z} - \frac{\partial \psi}{\partial z} \frac{\partial \phi'}{\partial x} - \frac{\partial \psi}{\partial x} \frac{d\phi_b}{dz} = D_B \nabla^2 \phi' + \frac{D_{Th}}{T_0} \nabla^2 T', \tag{76}$$

where v describes the local spinning motion of a continuum point observed in rotating frame of reference.

Introducing the nondimensional variables as in Eq. (16) and with $V = \frac{h}{\alpha_{bl}} v$ into the governing Eqs. (73)–(76), we get

$$\frac{1}{Pr_{nl}} \frac{\partial (\nabla^2 \Psi)}{\partial \tau} = a_1 \nabla^4 \Psi - a_1 \sqrt{Ta_{nl}} [1 + \epsilon^2 \delta_2 \cos(\omega \tau)] \frac{\partial V}{\partial Z} + Ra_{nl} a_1^2 \frac{\partial \Theta}{\partial X} - Ra_{\phi_{nl}} a_1^2 \frac{\partial \Phi}{\partial X}, \tag{77}$$

$$\frac{\partial V}{\partial \tau} = a_1 Pr_{nl} \left(\nabla^2 V + \sqrt{Ta_{nl}} [1 + \epsilon^2 \delta_2 \cos(\omega \tau)] \frac{\partial \Psi}{\partial Z} \right) - J(\Psi, V), \tag{78}$$

$$\frac{\partial \Theta}{\partial \tau} = a_1 \nabla^2 \Theta + \frac{\partial \Psi}{\partial X} - J(\Psi, \Theta), \tag{79}$$

$$\frac{\partial \Phi}{\partial \tau} = \frac{a_1}{Le_{nl}} \nabla^2 \Phi + \frac{a_1 N_{A_{nl}}}{Le_{nl}} \nabla^2 \Theta + \frac{\partial \Psi}{\partial X} - J(\Psi, \Phi), \tag{80}$$

where $Ta_{nl} = \left(\frac{2h^2 \rho_0 \Omega}{\mu_{nl}} \right)^2$ is the Taylor number which characterizes the rotation rate. Equations (77)–(80) are solved subject to stress-free, isothermal and iso-nanoparticles' concentration boundary conditions defined in Eq. (20).

Weakly nonlinear stability analysis

We make a weakly nonlinear stability analysis of the system by assuming the stream function, temperature and nanoparticles' concentration as in Eqs. (21)–(23) and for V , we assume:

$$V = \frac{\sqrt{2} a_1 \delta^2}{\pi^2} \mathcal{D}(\tau) \sin(\pi \kappa X) \cos(\pi Z) + \frac{\delta^3}{\pi^2} \mathcal{E} \sin(2\pi \kappa_c X). \tag{81}$$

Substituting Eqs. (21)–(23) and (79) in Eqs. (77)–(80) and taking the orthogonality condition with the eigenfunctions associated with the considered minimal modes, we get

$$\frac{d\mathcal{A}}{d\tau_1} = a_1 Pr_{nl} (\mathcal{B} - \mathcal{A} - ta_{nl} [1 + \epsilon^2 \delta_2 \cos(\omega^* \tau_1)] \mathcal{D} - r_{\phi_{nl}} \mathcal{L}), \tag{82}$$

$$\frac{d\mathcal{B}}{d\tau_1} = a_1 (r_{nl} \mathcal{A} - \mathcal{B} - \mathcal{A} \mathcal{C}), \tag{83}$$

$$\frac{d\mathcal{C}}{d\tau_1} = a_1 (\mathcal{A} \mathcal{B} - b_1 \mathcal{C}), \tag{84}$$

$$r_{nl} \frac{d\mathcal{L}}{d\tau_1} = a_1 \left(r_{nl} \mathcal{A} - \frac{N_{A_{nl}}}{Le_{nl}} \mathcal{B} - \frac{r_{nl}}{Le_{nl}} \mathcal{L} + r_{nl} \mathcal{A} \mathcal{M} \right), \tag{85}$$

$$r_{nl} \frac{d\mathcal{M}}{d\tau_1} = a_1 \left(\frac{b_1 N_{A_{nl}}}{Le_{nl}} \mathcal{C} - \frac{b_1 r_{nl}}{Le_{nl}} \mathcal{M} - r_{nl} \mathcal{A} \mathcal{L} \right), \tag{86}$$

$$\frac{d\mathcal{D}}{d\tau_1} = a_1 (Pr_{nl} ta_{nl} [1 + \epsilon^2 \delta_2 \cos(\omega^* \tau_1)] \mathcal{A} - Pr_{nl} \mathcal{D}) - \mathcal{A} \mathcal{E}, \tag{87}$$

$$\frac{d\mathcal{E}}{d\tau_1} = -d a_1 Pr_{nl} \mathcal{E} + a_1^2 \mathcal{A} \mathcal{D}, \tag{88}$$

where $d = \kappa^2 b_1$ and $ta_{nl} = \sqrt{\frac{Ta_{nl} \pi^2}{\delta^6}}$.

We now use the following regular perturbation expansion in Eqs. (82)–(88) in addition to small time scale and a weak thermophoretic effect:

$$\begin{bmatrix} \mathcal{A} \\ \mathcal{B} \\ \mathcal{C} \\ \mathcal{L} \\ \mathcal{M} \\ \mathcal{D} \\ \mathcal{E} \\ r_{nl} \end{bmatrix} = \begin{bmatrix} 0 \\ 0 \\ 0 \\ 0 \\ 0 \\ 0 \\ 0 \\ r_0 \end{bmatrix} + \epsilon \begin{bmatrix} A_1 \\ B_1 \\ C_1 \\ L_1 \\ M_1 \\ D_1 \\ E_1 \\ 0 \end{bmatrix} + \epsilon^2 \begin{bmatrix} A_2 \\ B_2 \\ C_2 \\ L_2 \\ M_2 \\ D_2 \\ E_2 \\ r_2 \end{bmatrix} + \epsilon^3 \begin{bmatrix} A_3 \\ B_3 \\ C_3 \\ L_3 \\ M_3 \\ D_3 \\ E_3 \\ 0 \end{bmatrix} + \dots \quad (89)$$

Following the procedure of Sec. (2.3), we can get the Ginzburg–Landau equation in the form:

$$\frac{dA_{1_0}(\tau_1^*)}{d\tau_1^*} = Q_5 A_{1_0}(\tau_1^*) - Q_6 A_{1_0}^3(\tau_1^*), \quad (90)$$

where

$$\left. \begin{aligned} Q_5 &= \frac{a_1 \text{Pr}_{nl} [r_2 + N_{A_{nl}} r_{\phi_{nl}} - 2\delta_2 \cos(\omega^* \tau_1^*) \text{ta}_{nl}^2]}{1 + \text{Pr}_{nl}(r_0 - \text{Le}_{nl}^2 r_{\phi_{nl}}) - \text{ta}_{nl}^2} \\ Q_6 &= \frac{\left[a_1 \text{Pr}_{nl}(r_0 - \text{Le}_{nl}^3 r_{\phi_{nl}}) - \frac{a_1 b_1 \text{ta}_{nl}^2}{d \text{Pr}_{nl}} \right]}{b_1 [1 + \text{Pr}_{nl}(r_0 - \text{Le}_{nl}^2 r_{\phi_{nl}}) - \text{ta}_{nl}^2]} \end{aligned} \right\} \quad (91)$$

The Ginzburg–Landau equations (39), (71) and (90) obtained from gravity, boundary temperature and rotation modulations, respectively, are analytically intractable due to their non-autonomous nature. The coefficient of the linear term of the Ginzburg–Landau equations depends on amplitude and frequency of modulation. r_0 and r_2 in the Ginzburg–Landau equations (39), (71) and (88) are scaled Rayleigh number and scaled correction Rayleigh number. Without loss of generality, we assume $r_0 = r_c$, critical Rayleigh number for unmodulated system, and from previous investigation [7] we found that $r_2 \simeq 1$. We use Mathematica 8.0 to numerically solve the Ginzburg–Landau equations by using the initial condition $A_{1_0}(0) = 1$. Using this solution, we next quantify the heat transport in terms of the Nusselt number.

Estimation of heat transport at lower plate

The thermal Nusselt number, $\text{Nu}_{nl}(\tau_1^*)$, is defined as:

$$\text{Nu}_{nl}(\tau_1^*) = 1 + \frac{k_{nl}}{k_{bl}} \left[\frac{\int_0^{\frac{2\pi}{\pi\kappa_c}} \left(\frac{\partial \Theta}{\partial Z} \right) dX}{\int_0^{\frac{2\pi}{\pi\kappa_c}} \left(\frac{d\Theta_b}{dZ} \right) dX} \right]_{Z=0}, \quad (92)$$

where $\Theta_b = \frac{T_b - T_0}{\Delta T}$. Substituting Eqs. (10) and (22) in Eq. (92) and completing the integration, we get

$$\text{Nu}_{nl}(\tau_1^*) = 1 + \left(\frac{k_{nl}}{k_{bl}} \right) \frac{2}{r_{nl}} C(\tau_1^*). \quad (93)$$

Using first- and second-order solutions of $C(\tau_1^*)$, we get

$$\text{Nu}_{nl}(\tau_1^*) = 1 + \frac{2}{b_1} \left(\frac{k_{nl}}{k_{bl}} \right) \left(1 - \frac{1}{r_{nl}} \right) A_{1_0}(\tau_1^*)^2. \quad (94)$$

The time-averaged Nusselt number (mean Nusselt number), $\overline{\text{Nu}_{nl}(\tau_1^*)}$, for Eq. (94) is given by:

$$\overline{\text{Nu}_{nl}(\tau_1^*)} = \frac{1}{\left(\frac{2\pi}{\omega^*} \right)} \int_0^{\frac{2\pi}{\omega^*}} \text{Nu}_{nl}(\tau_1^*) d\tau_1^*. \quad (95)$$

From Eq. (95), it is clear that the mean Nusselt number is calculated in the interval $\left[0, \frac{2\pi}{\omega^*} \right]$. The amplitude, $A_{1_0}(\tau_1^*)$, in Eq. (94) is the solution of the Ginzburg–Landau equations (39), (71) and (90) of gravity, boundary temperature and rotation modulations, respectively. Using this solution, we calculate the mean Nusselt number for different values of amplitude and frequency of modulation.

Results and discussion

The individual effect of time-periodic modulations of the gravity field, boundary temperature and the rotation of the channel on Rayleigh–Bénard convection in nanoliquids is studied in the paper using the generalized Buongiorno two-phase model. Using a truncated Fourier series representation, the generalized Lorenz model is derived for all the three modulated problems. Method of multiscales is then employed to reduce the Lorenz model into a Ginzburg–Landau model. Using the Ginzburg–Landau equation, the amplitude is obtained numerically and the Nusselt number is evaluated as a quadratic function of the amplitude. The results and their discussion is focused mainly on the following aspects:

1. Studying the influence of nanoparticles (nanotubes) on heat transport in the presence/absence of modulation.
2. Discussing the effect of gravity, boundary temperature and rotational modulations on heat transport in Newtonian liquids and Newtonian nanoliquids.
3. Explaining the individual effects of three types of modulation and comparing them.
4. Recovering results of single-phase model from those of two-phase.
5. Qualitative comparison of the present results with those of previous experimental and numerical works.

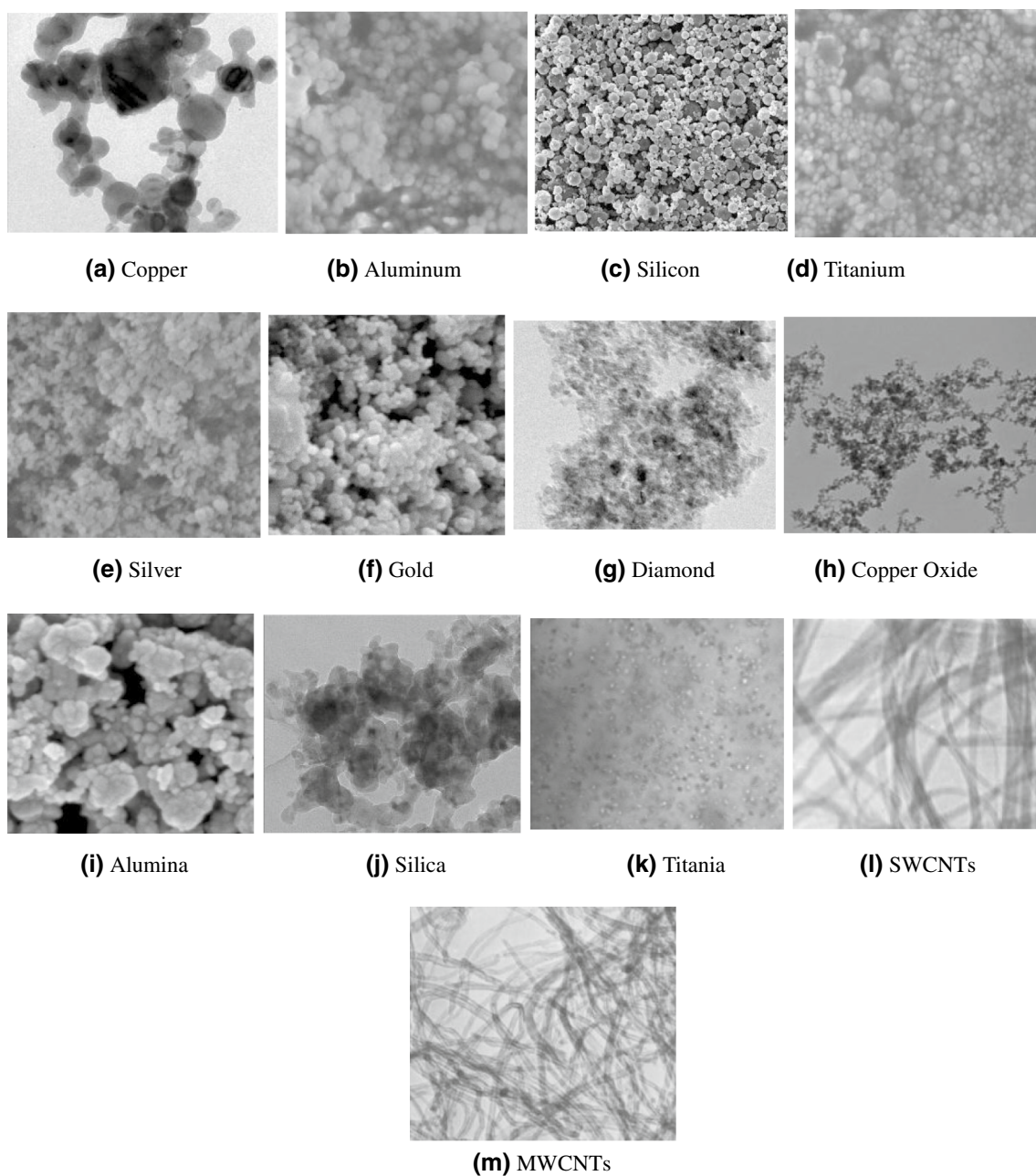


Fig. 5 The transmission electron microscope (TEM) pictures of nanoparticles and nanotubes in >100 nm size [44]

Table 2 Thermophysical properties of four base liquids at 300° K [43]

Baseliquids	μ_{bl}	ρ_{bl}	k_{bl}	$\beta_{bl} \times 10^5$	$C_{p_{bl}}$
Water (W)	0.00089	997	0.613	21	4179
Ethylene glycol (E-G)	0.0157	1114.4	0.252	65	2415
Engine oil (E-O)	0.486	884	0.144	70	1910
Glycerin (G)	0.799	1259.9	0.286	48	2427

Table 3 Thermophysical properties of five nanoparticles at 300° K [43]

Nanoparticles	ρ_{np}	k_{np}	$\beta_{np} \times 10^5$	$C_{p_{np}}$
Copper (Cu)	8933	401	1.67	385
Copper oxide (CuO)	6320	76.5	1.8	531.8
Silver (Ag)	10,500	429	1.89	235
Alumina (Al ₂ O ₃)	3970	40	0.85	765
Titania (TiO ₂)	4250	8.9538	0.9	686.2

Table 4 Thermophysical properties of carbon nanotubes at 300° K [43]

Nanotubes	ρ_{np}	k_{np}	$\beta_{np} \times 10^5$	C_{pnp}
SWCNTs	2600	6600	0.16	425
MWCNTs	2640	15	2.1	730

Influence of nanoparticles (nanotubes) on heat transport in the presence/absence of modulation

The Nusselt number for four Newtonian liquids ($\chi = 0$) and for twenty-eight Newtonian nanoliquids ($\chi = 0.05$) are presented. Twenty-eight Newtonian nanoliquids are studied by making a combination of four Newtonian liquids with five nanoparticles and two nanotubes. The transmission electron microscope (TEM) pictures of these nanoparticles (nanotubes) of size >100 nm are shown in Fig. 5. The actual physical values of Newtonian liquids, nanoparticles and nanotubes are used in the study. Their thermophysical properties are tabulated in Tables 2–4. Tables 2–4 clearly show that the thermal conductivity of all Newtonian liquids is less than 1 whereas the nanoparticles made from metals and metal oxides and carbon nanotubes have their thermal conductivity in the range 8 to 6600. The feasibility study on these eleven nanoparticles and two carbon nanotubes is explained well by Kanchana and Zhao [43]. They argued that enhanced heat transport in Newtonian liquids due to nanoparticles (nanotubes) not only depends on thermal

conductivity of nanoparticles (nanotubes) but also the contribution of other thermophysical properties of nanoparticles (nanotubes) also counts.

It is pretty clear from Table 5 that smaller the particle size, greater the surface area and hence better the particle activity. Thus, in this sense the nanoparticles are very sensitive than the microparticles. In fact, the thermal instability is lower for the nanoliquid compared to the base liquid [45]. Therefore, nanoparticles (nanotubes) have to be dispersed in the base liquid very gently, there should be no violent vibration and friction. They should also be protected from moisture, heat and sunlight. Nanoparticles possess an attractive force and such a force becomes stronger as size decreases and hence there will be a maximum possibility of agglomeration. To avoid agglomeration, varieties of surfactants are being used [46]. The stability of nanoparticles in base liquid depends heavily on the surfactants, the base liquid, size of particles and molecular weight. For example, the stability of colloidal copper in Ethylene glycol and Engine oil is retained for a longer time when compared to that in water [47, 48]. With this brief information on nanoparticles, we now see the influence of nanoparticles on heat transport using the non-dimensional parameters which characterize the nanoliquid properties.

The values of nondimensional parameters, Prandtl number (Pr), modified diffusivity ratio (N_{Anl}), Lewis number (Le_{nl}) and nanoparticle concentration Rayleigh number ($Ra_{\phi_{nl}}$) for different nanoliquids are documented in Table 6 for $\chi = 0.05$. It is apparent from this table that the effect of

Table 5 Details of material in nano size as per US Research Nanomaterials, Inc [44]

Material	APS	SSA/m ²	Color	Purity	Price/gm	Economical feasibility
Copper	40 nm	45	Dark brown	99.9%	\$ 35	Reasonably priced
Aluminum	40 nm	30–50	Dark gray	> 99.9%	\$35	Reasonably priced
Silicon	10 nm	185	Red brown	> 98%	\$59	Highly expensive
Titanium	30–50 nm	50	White	99.9%	\$45	Highly expensive
Silver	20 nm	18–22	Black	99.99%	\$25	Reasonably priced
Gold	15 nm	–	Dark brown	99.95%	\$225	Highly expensive
Diamond	3–10 nm	272.63	Gray	54.5%	\$45	Highly expensive
Copper oxide	10 nm	85	Brown black	99%	\$10.6	Less expensive
Alumina	5 nm	> 150	White	99.99%	\$18	Less expensive
Silica	8 nm	185	White	99%	\$7.8	Less expensive
Titania	5 nm	289	White	99.5%	\$ 7.4	Less expensive
SWCNTs	OD = 1–2 nm ID = 0.8–1.6 nm L=15–50 μ m	580	Black	60%	\$ 208	Highly expensive
MWCNTs	OD < 7 nm ID = 2–5 nm L=10–30 μ m	500	Black	95%	\$ 39	Highly expensive

APS average particles size, SSA specific surface area, OD outer diameter, ID inner diameter, L length

Table 6 Values of various parameters concerning twenty-eight nanoliquids for volume fraction, $\chi = 0.05$, at 300° K

Nanoliquids	Pr_{nl}	$N_{A_{nl}}$	Le_{nl}	$Ra_{\phi_{nl}}$
W-Cu	4.22677	4.27688	2.65408	2.86351
W-CuO	4.67228	4.69714	2.64933	2.86864
W-Ag	3.95458	4.04957	2.68579	2.82970
W-Al ₂ O ₃	5.14669	5.15275	2.65177	2.86600
W-TiO ₂	5.17765	4.93780	2.60410	2.91848
W-SWCNT	5.31137	5.53994	2.73295	2.78087
W-MWCNT	5.44366	5.59635	2.66160	2.93034
EG-Cu	110.90618	4.42910	2.59585	2.92775
EG-CuO	121.41153	4.84051	2.59660	2.92690
EG-Ag	103.54036	4.21010	2.64296	2.87557
EG-Al ₂ O ₃	132.13750	5.28144	2.60882	2.91320
EG-TiO ₂	131.54540	5.14775	2.59170	2.93244
EG-SWCNT	134.40910	5.77106	2.71252	2.86709
EG-MWCNT	137.25121	4.96770	2.65189	3.13951
EO-Cu	4575.17633	4.08368	2.50248	3.03698
EO-CuO	5084.45057	4.54025	2.50637	3.03227
EO-Ag	4194.50616	3.84931	2.57290	2.95387
EO-Al ₂ O ₃	5612.21209	5.04781	2.52764	3.00676
EO-TiO ₂	5547.15282	4.93821	2.52326	3.01197
EO-SWCNT	5669.37919	4.42065	2.67889	2.45609
EO-MWCNT	5821.39785	4.95978	2.60356	1.74361
G-Cu	5136.36918	4.58597	2.61551	2.90574
G-CuO	5580.03308	4.97093	2.61547	2.90579
G-Ag	4825.16267	4.37745	2.65752	2.85981
G-Al ₂ O ₃	6026.70821	5.37629	2.62553	2.89465
G-TiO ₂	6014.39828	5.23688	2.60477	2.91772
G-SWCNT	6119.03328	5.52541	2.71941	2.71154
G-MWCNT	6243.77484	4.52748	2.66107	2.45517

nanoparticles (nanotubes) is to reduce the Prandtl number and enhance the nanoparticle concentration Rayleigh number, Lewis number and thermal diffusivity ratio. All these nondimensional parameters characterize the nanoliquid properties. We now try to understand the influence of these parameters on heat transport.

Prandtl number correlates the momentum transport and the thermal transport. Decrease in Prandtl number essentially means that the thermal transport dominates over the momentum transport and hence facilitates the heat transfer. Lewis number correlates the mass transport and the thermal transport. Increase in Lewis number due to nanoparticles (nanotubes) in base liquid means that the thermal transport dominates over the mass transport which improves the heat transfer much better. The modified diffusivity ratio signifies

Table 7 Nusselt number of twenty-eight nanoliquids for different values of volume fraction, χ , calculated using the Nusselt number for water = 2.00332, ethylene-glycole = 2.05386, engine oil = 2.05615 and glycerin = 2.05615

Nanoliquids	$\chi = 0.03$	% of enhancement	$\chi = 0.05$	% of enhancement
W-Cu	2.19242	9.44	2.28853	14.24
W-CuO	2.19771	9.70	2.29738	14.68
W-Ag	2.19092	9.36	2.28666	14.14
W-Al ₂ O ₃	2.20313	9.97	2.30692	15.15
W-TiO ₂	2.18242	8.94	2.26972	13.30
W-SWCNT	2.25718	12.67	2.40561	20.08
W-MWCNT	2.22816	11.22	2.35177	17.39
EG-Cu	2.27243	10.64	2.38236	15.99
EG-CuO	2.27490	10.76	2.38622	16.18
EG-Ag	2.27626	10.83	2.39035	16.38
EG-Al ₂ O ₃	2.27866	10.95	2.39284	16.50
EG-TiO ₂	2.26883	10.47	2.37513	15.64
EG-SWCNT	2.33555	13.72	2.49712	21.58
EG-MWCNT	2.31773	12.85	2.46343	19.94
EO-Cu	2.26222	10.02	2.36170	14.86
EO-CuO	2.26580	10.20	2.36719	15.13
EO-Ag	2.26907	10.36	2.37523	15.52
EO-Al ₂ O ₃	2.27163	10.48	2.37724	15.62
EO-TiO ₂	2.26631	10.22	2.36779	15.16
EO-SWCNT	2.33396	13.51	2.49108	21.15
EO-MWCNT	2.31848	12.76	2.46153	19.72
G-Cu	2.27976	10.88	2.39329	16.40
G-CuO	2.28156	10.96	2.39606	16.53
G-Ag	2.28324	11.04	2.40055	16.75
G-Al ₂ O ₃	2.28445	11.10	2.40122	16.78
G-TiO ₂	2.27327	10.56	2.38102	15.80
G-SWCNT	2.34045	13.83	2.50393	21.78
G-MWCNT	2.32150	12.91	2.46819	20.04

the relative importance of thermophoresis (Soret-type cross-diffusion) and molecular diffusion. Increase in the value of the modified thermal diffusivity ratio means thermophoresis has increasing influence on heat transport with an improvement in it. The nanoparticle concentration Rayleigh number is the analog of the thermal Rayleigh number, and this correlates the buoyancy force due to concentration difference and viscous force. Increase in the value of the concentration Rayleigh number means that the buoyancy force due to concentration becomes more important than the viscous force and this also favors enhanced heat transfer. Thus the perception from the above results is that the influence of

Table 8 Values of \overline{Nu}_{nl} for twenty-eight Newtonian nanoliquids for different values of δ_2 , ω^* and for $\chi = 0.05$ in the case of gravity modulation

Nanoliquids	$\delta_2 = 0.1$ $\omega^* = 5$	$\delta_2 = 0.2$ $\omega^* = 5$	$\omega^* = 8$ $\delta_2 = 0.1$
W	2.02044	2.03803	1.87560
EG	2.07187	2.09042	1.91627
EO	2.07419	2.09277	1.91817
G	2.07419	2.09277	1.91817
W-Cu	2.31045	2.33301	2.09853
W-CuO	2.31935	2.34198	2.10483
W-Ag	2.30861	2.33120	2.09714
W-Al ₂ O ₃	2.32894	2.35163	2.11162
W-TiO ₂	2.29116	2.31323	2.08118
W-SWCNT	2.42910	2.45333	2.19166
W-MWCNT	2.37445	2.39781	2.14770
EG-Cu	2.40501	2.42840	2.17757
EG-CuO	2.40884	2.43221	2.18003
EG-Ag	2.41309	2.43658	2.18461
EG-Al ₂ O ₃	2.41545	2.43880	2.18474
EG-TiO ₂	2.39751	2.42063	2.17000
EG-SWCNT	2.52083	2.54537	2.27222
EG-MWCNT	2.48681	2.51100	2.24375
EO-Cu	2.38418	2.40739	2.16123
EO-CuO	2.38967	2.41287	2.16492
EO-Ag	2.39786	2.42123	2.17286
EO-Al ₂ O ₃	2.39974	2.42297	2.17230
EO-TiO ₂	2.39017	2.41327	2.16451
EO-SWCNT	2.51474	2.53924	2.26765
EO-MWCNT	2.48495	2.50917	2.24262
G-Cu	2.41598	2.43943	2.18665
G-CuO	2.41872	2.44213	2.18824
G-Ag	2.42331	2.44684	2.19312
G-Al ₂ O ₃	2.42385	2.44724	2.19180
G-TiO ₂	2.40340	2.42652	2.17494
G-SWCNT	2.52763	2.55217	2.27821
G-MWCNT	2.49155	2.51571	2.24794

nanoparticles (nanotubes) in base liquid is to enhance heat transport. The percentage of enhancement of heat transport due to nanoparticles (nanotubes) in base liquid is presented in Table 7.

The values of mean Nusselt number for twenty-eight nanoliquids at different volume fractions of nanoparticles (nanotubes) in the absence of modulation are documented in Table 7. From Table 7, it is clear that dilute concentrations of nanoparticles (nanotubes) in base liquids lead to a significant increase in heat transfer. Maximum heat transfer enhancement is noticed in glycerin-based SWCNTs while the minimum one is in water-based titania nanoparticles.

Tables 8–10 present values of the mean Nusselt number for gravity, boundary temperature and rotational modulations for Newtonian liquids and Newtonian nanoliquids. These tables reiterate the results of the no-modulation problem, viz., nanoparticles (nanotubes) in base liquid enhance the heat transport irrespective of the values of amplitude and frequency of modulation. There is quite a change in the value of the mean Nusselt number due to modulations and this is discussed in the succeeding subsection.

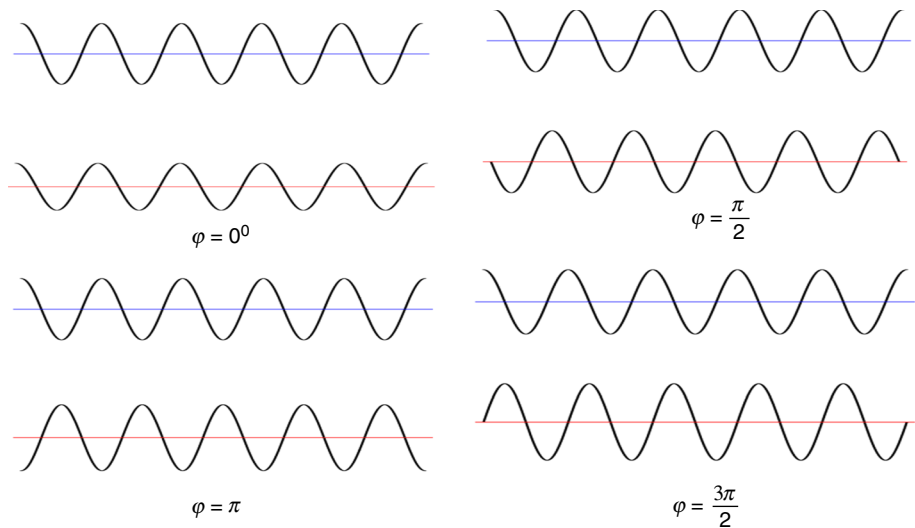
Results from modulation

When a time-periodic modulation is imposed on a Rayleigh–Bénard convection system involving Newtonian liquids or Newtonian nanoliquid layers, then the flow in the system gets disturbed. The rate of heat transport in such a system thereby alters. In the past few decades, different types of modulation in hydrodynamics have been studied with great interest. The interest lies not only in the mechanics of this new class of problems but also with the immense possibilities for applications, e.g., using modulation, enhancement of heat transport or higher efficiency can be attained in various processing techniques. The present paper is an attempt to study the individual effect of three types of modulations on heat transport and seek the merits and demerits of such modulations. The three types of modulations considered in the paper are:

1. Gravity modulation,
2. Boundary temperature modulation and
3. Rotational modulation.

We now discuss the effect of gravity modulation on heat transport in the Rayleigh–Bénard convection problem involving Newtonian liquids or Newtonian nanoliquids. When such liquid layer vibrates vertically with small amplitude, $\epsilon^2 \delta_2$ and low frequency, ω^* , their momentum and heat transports modifies. The values of the average Nusselt number for four Newtonian liquids and twenty-eight Newtonian nanoliquids for different values of δ_2 and ω^* are documented in Table 8. From Table 8, it is clear that the effect of increase in the amplitude of modulation is to increase the mean Nusselt number whereas the effect of increase in frequency of modulation is to decrease the same. Comparing Table 8 with Table 7, it is apparent that at $\omega^* = 5$ the effect of gravity modulation is to enhance heat transport of the system. However, when ω^* increases in value slightly beyond 5 it has an opposing influence. Thus, if we choose gravity modulation as a regulating mechanism of heat transfer in any application frequency of modulation is a dominant factor than the amplitude.

Fig. 6 Schematic of in-phase and out-of-phase temperature modulations for a cosine function of time and for four different values of phase difference, φ



Let us now move on to the discussion of the effect of boundary temperature modulation. The present work focuses on two types of boundary temperature modulations:

1. In-phase modulation (synchronous) and
2. Out-of-phase modulation (asynchronous).

$\varphi = 0^\circ$ represents in-phase modulation and $\varphi \neq 0^\circ$ represents the out-of-phase modulation. The schematic of in-phase and out-of-phase modulations for cosine function is shown in Fig. 6. The values of mean Nusselt number for Newtonian liquids and Newtonian nanoliquids for in-phase and out-of-phase temperature modulations are documented in Table 9. From the table, it is clear that there is no influence of modulation in the case of in-phase modulation. Further, modulation has less influence in the case when the phase difference is $\varphi = \pi$. The effect of the amplitude on mean Nusselt number as a function of the phase difference for four different frequencies ($\omega^* = 0.6, 1, 3$ and 5) is shown in Fig. 7. It can be easily seen that the mean Nusselt number decreases with increase in frequency. The effect of increase in phase difference is to decrease \overline{Nu}_{nl} in $[0, \pi]$ while it increases with φ in $[\pi, 2\pi]$. When the phase difference takes the values $\varphi = \frac{\pi}{2}$ and $\varphi = \frac{3\pi}{2}$ the effect of boundary temperature modulation is most significant. When the results documented in Table 9 are seen in conjunction with the schematic in Fig. 6, we may conclude that:

1. Odd multiples of $\frac{\pi}{2}$ have significant effect and even multiples of $\frac{\pi}{2}$ do not have or have less influence on the heat transport and

Table 9 Variation of \overline{Nu}_{nl} in the case of in-phase and out-of-phase temperature modulations for $r_{nl} = 5, \delta_2 = 0.1, \omega^* = 5$

Nanoliquid	In-phase modulation $\varphi = 0$	Out-of-phase modulation		
		$\varphi = \frac{\pi}{2}$	$\varphi = \pi$	$\varphi = \frac{3\pi}{2}$
W	2.00332	2.01323	1.99849	1.98868
EG	2.05386	2.06371	2.04749	2.03775
EO	2.05615	2.06598	2.04970	2.03997
G	2.05615	2.06599	2.04971	2.03997
W-Cu	2.28853	2.30049	2.28007	2.26823
W-CuO	2.29738	2.30927	2.28866	2.27690
W-Ag	2.28666	2.29864	2.27820	2.26635
W-Al ₂ O ₃	2.30692	2.31871	2.29790	2.28624
W-TiO ₂	2.26972	2.28134	2.26123	2.24974
W-SWCNTs	2.40561	2.41764	2.39484	2.38297
W-MWCNTs	2.35177	2.36363	2.34190	2.33018
EG-Cu	2.38236	2.39362	2.37113	2.36002
EG-CuO	2.38622	2.39743	2.37493	2.36387
EG-Ag	2.39035	2.40151	2.37879	2.36779
EG-Al ₂ O ₃	2.39284	2.40397	2.38140	2.37042
EG-TiO ₂	2.37513	2.38622	2.36395	2.35301
EG-SWCNTs	2.49712	2.50806	2.48360	2.47283
EG-MWCNTs	2.46343	2.47448	2.45064	2.43975
EO-Cu	2.36170	2.37316	2.35113	2.33982
EO-CuO	2.36719	2.37861	2.35654	2.34527
EO-Ag	2.37523	2.38653	2.36412	2.35297
EO-Al ₂ O ₃	2.37724	2.38856	2.36635	2.35518
EO-TiO ₂	2.36779	2.37907	2.35701	2.34588
EO-SWCNTs	2.49108	2.50208	2.47773	2.46691
EO-MWCNTs	2.46153	2.47271	2.44894	2.43792
G-Cu	2.39329	2.40443	2.38174	2.37076
G-CuO	2.39606	2.40717	2.38448	2.37353
G-Ag	2.40055	2.41159	2.38870	2.37781
G-Al ₂ O ₃	2.40122	2.41225	2.38952	2.37864
G-TiO ₂	2.38102	2.39201	2.36962	2.35878
G-SWCNTs	2.50393	2.51477	2.49022	2.47955
G-MWCNTs	2.46819	2.47914	2.45522	2.44444

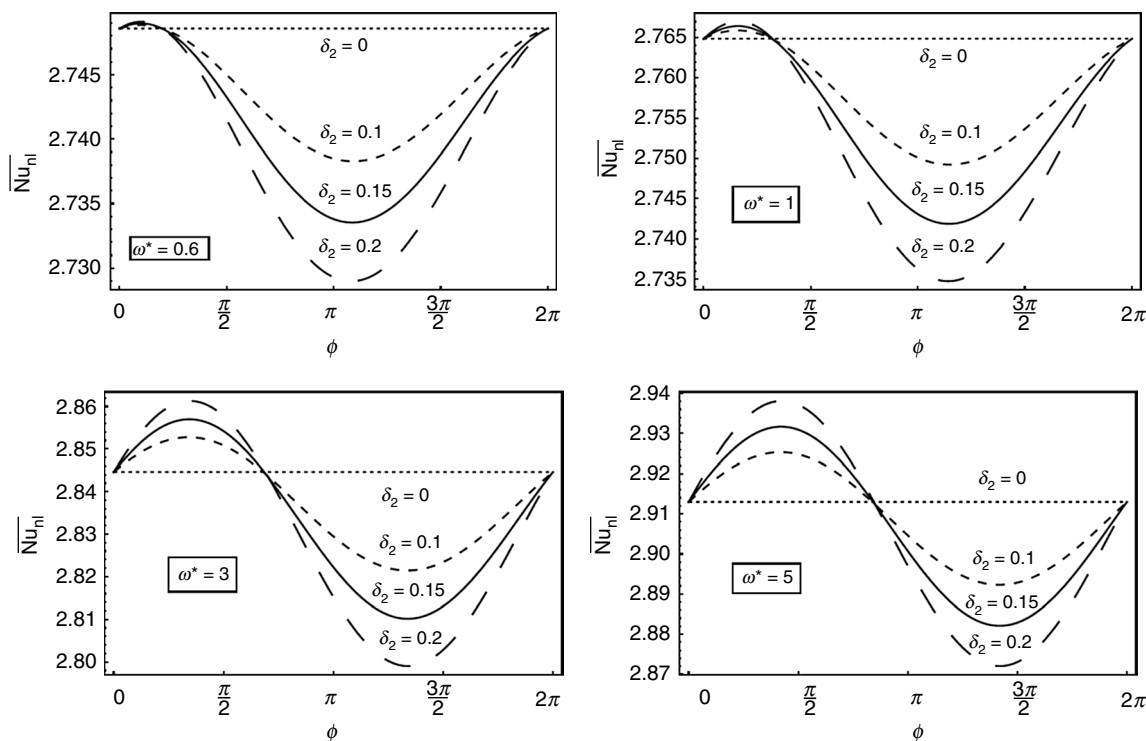


Fig. 7 Variation of $\overline{Nu_{ni}}$ with phase difference ϕ for water–copper nanoliquid and for different values of δ_2 and for ω^*

- the modulation is significant when there is a phase-lag of the sinusoidal temperature at the lower plate compared to that at the upper plate.

This suggests that in-phase modulation cannot be used to regulate heat transport and this result is true for all Newtonian liquids and Newtonian nanoliquids (see Table 9). Thus, the choice of phase difference and frequency of modulations are very important factors in the case of boundary temperature modulation.

Rotational modulation is achieved by rotating the liquid layer uniformly about the fixed axis of Z. Taylor number characterizes the rotation rate. Table 10 shows the values of the mean Nusselt number in the presence/absence of rotational modulation for Newtonian liquids and Newtonian nanoliquids for a value of $Ta_{nl} = 100$ and for different values of ω^* and δ_2 . From the tables, it is apparent that the effect of small values of δ_2 is to enhance the heat transport whereas the effect of increasing ω^* is to diminish the same. The rate of enhancement due to amplitude is less than the rate of diminishment due to frequency of rotational modulation. Figure 8 is the plot of $\overline{Nu_{ni}}$ versus scaled Rayleigh

number, r_{nl} , for different values of Ta_{nl} for a representative nanoliquid, viz., water–copper nanoliquid. Figure 8 reveals that as we increase Ta_{nl} , $\overline{Nu_{ni}}$ decreases which implies that the effect of rotation is to diminish heat transport. Overall, we conclude that the frequency of modulation and the Taylor number are dominant parameters that influence heat transport the most in the case of rotational modulation.

Explanation for the observed individual effects of three types of modulations

On observing the coefficient of the linear term in the algebraic part of the Ginzburg–Landau equations (39), (69) and (88) of gravity, temperature and rotation modulations, respectively, one can easily see that the modulation-related quantities appear only in this term. The quantities Q_1, Q_3 and Q_5 are growth-related terms while Q_2, Q_4 and Q_6 play their designated role of keeping the solution bounded. It is thus fairly clear that a closer inspection of Q_1, Q_3 and Q_5 would throw more light on the effect of modulation on the amplitude and thereby the Nusselt number. Figure 9 is a plot of

Table 10 Values of \overline{Nu}_{nl} for twenty-eight Newtonian nanoliquids for different values of δ_2 , ω^* and for $\chi = 0.05$ in the presence rotation modulation

Nanoliquids	$\delta_2 = 0.1$ $\omega^* = 5$	$\delta_2 = 0.2$ $\omega^* = 5$	$\omega^* = 8$ $\delta_2 = 0.1$
W	1.94166	1.94292	1.85383
EG	1.96191	1.96336	1.86992
EO	1.96281	1.96426	1.87065
G	1.96281	1.96426	1.87065
W-Cu	2.18114	2.18306	2.05115
W-CuO	2.18397	2.18591	2.05280
W-Ag	2.18124	2.18316	2.05127
W-Al ₂ O ₃	2.18732	2.18930	2.05480
W-TiO ₂	2.15664	2.15853	2.02856
W-SWCNT	2.26444	2.26670	2.11987
W-MWCNT	2.22095	2.22306	2.08290
EG-Cu	2.21680	2.21901	2.08096
EG-CuO	2.21883	2.22105	2.08211
EG-Ag	2.22170	2.22395	2.08513
EG-Al ₂ O ₃	2.22253	2.22478	2.08457
EG-TiO ₂	2.20839	2.21059	2.07241
EG-SWCNT	2.30033	2.30289	2.15089
EG-MWCNT	2.27561	2.27806	2.12978
EO-Cu	2.20303	2.20515	2.07025
EO-CuO	2.20636	2.20849	2.07241
EO-Ag	2.21124	2.21343	2.07707
EO-Al ₂ O ₃	2.21245	2.21462	2.07676
EO-TiO ₂	2.20471	2.20687	2.07012
EO-SWCNT	2.29564	2.29817	2.14726
EO-MWCNT	2.27515	2.27758	2.12996
G-Cu	2.22254	2.22480	2.08554
G-CuO	2.22392	2.22618	2.08617
G-Ag	2.22693	2.22922	2.08931
G-Al ₂ O ₃	2.22671	2.22899	2.08792
G-TiO ₂	2.21065	2.21288	2.07409
G-SWCNT	2.30362	2.30620	2.15364
G-MWCNT	2.27716	2.27964	2.13098

Q_1, Q_3 and Q_5 versus τ_1^* for a fixed value of the parameters appearing in them. The figure clearly reveals that

$$\overline{Q}_1 > \overline{Q}_3 > \overline{Q}_5. \tag{94}$$

On seeing this result in conjunction with those of the average Nusselt number, we may conclude that the Nusselt number is highest for gravity modulation for which the mean, \overline{Q}_1 is highest. It is obvious that the one with the maximum area under the curve has maximum heat transfer.

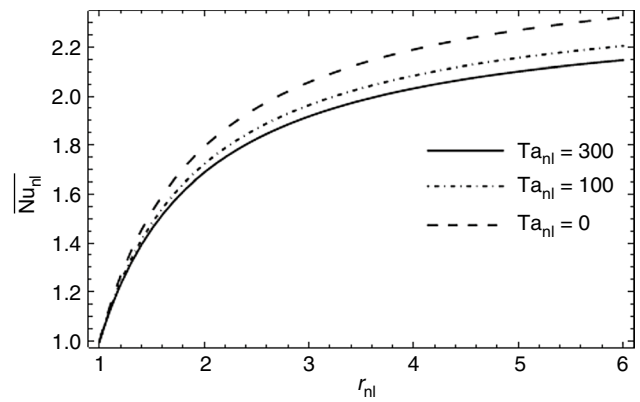


Fig. 8 Plots of \overline{Nu}_{nl} versus r_{nl} for water–copper nanoliquid and different values of Ta_{nl} and for $r_{nl} = 5, \delta_2 = 0.1$ and $\omega^* = 5$

We made similar computation with Q_2, Q_4 and Q_6 and these reiterate what is said above.

Recovering results of single-phase model from those of two-phase

As mentioned in the introduction to the paper, the generalized Buongiorno two-phase model allows one to deduce the results of the single-phase model from that of the two-phase. Siddheshwar and Kanchana [31, 32] showed that the results pertaining to single-phase model [49–53] and references therein) can be recovered as a limiting case of the generalized Buongiorno two-phase model by taking nanoparticles concentration Rayleigh number, $Ra_{\phi_{nl}} = 0$. In the present paper, we found that the results of Siddheshwar and Kanchana [31, 32] are true in the presence of modulation also (see Fig. 10).

Qualitative comparison of the present results with those of previous experimental and numerical works

The experimental findings of Swaminathan et al. [54], Niemela Donnelly [55] and Niemela et al. [56] and the numerical findings of Gresho and Sani [2] and Elhajjar et al. [57] on Rayleigh–Bénard convection in the presence/absence of different types of modulations for rigid boundaries are summarized in Table 11. From previous investigations [31, 32, 58, 59], we know that in the presence/absence of nanoparticles:

$$Nu^{[FF]} > Nu^{[RR]}, \tag{97}$$

and

Fig. 9 Variation of Q_1, Q_3 and Q_5 with time for $\delta_2 = 0.1, \omega^* = 5, \chi = 0.05$ and $r_{nl} = 5$

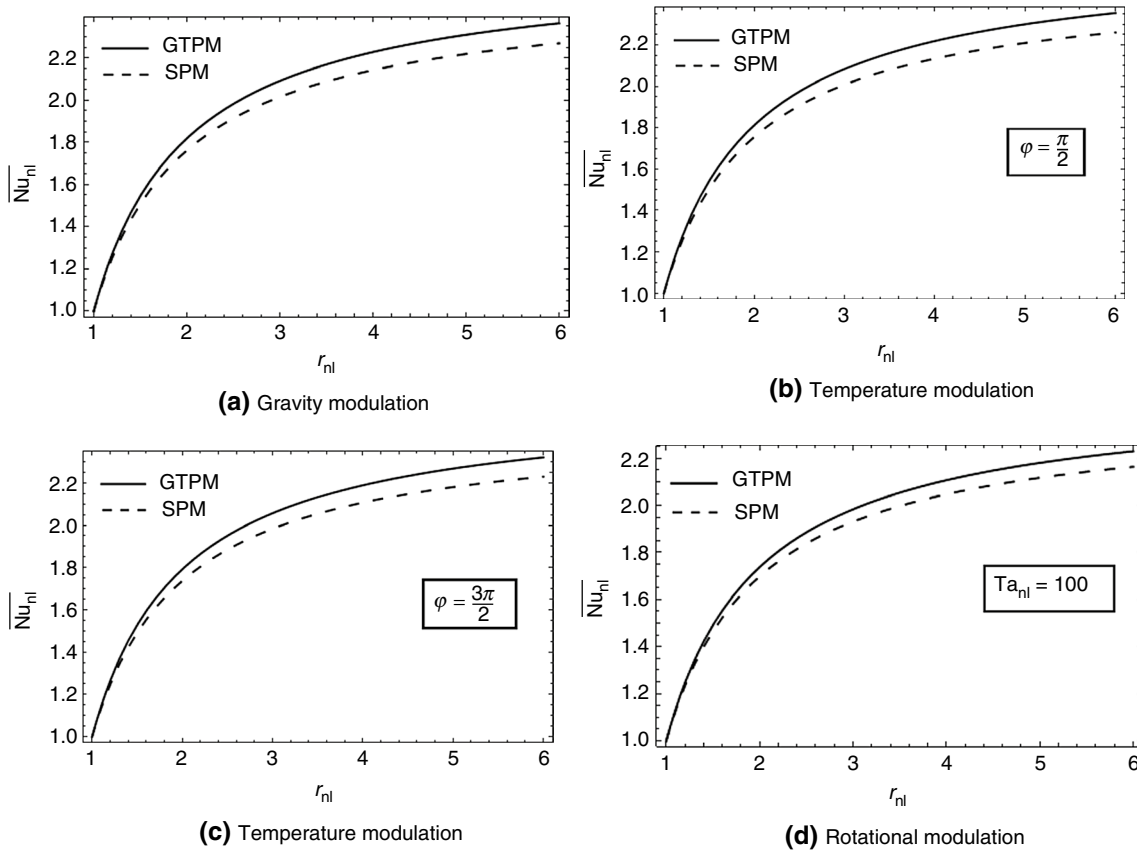
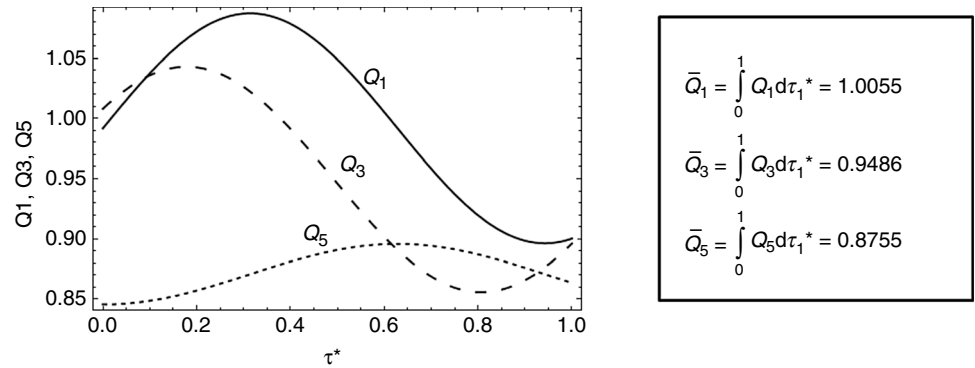


Fig. 10 Variation of $\overline{Nu_{nl}}$ with r_{nl} for water–copper nanoliquid and for $\delta_2 = 0.1$ and for $\omega^* = 5$ for gravity, temperature and rotational modulations

$$Nu_{nl}^{[\text{Rectangular enclosure}]} < Nu_{nl}^{[\text{Classical RBC}]}, \tag{98}$$

where FF and RR, respectively, represent the free boundaries and the rigid boundaries.

In the present investigation, we obtained $Nu_{nl} = 2.8507 (> 1.586)$ for water–alumina nanoliquids in the absence of modulations at volume fraction, $\chi = 0.08$.

These satisfies the relation (98) implying the present investigation is in reasonably good agreement with previous investigation.

Though we have made a qualitative comparison of results obtained in the present study with previous investigations, some of these remains to be experimentally proven, more so because all the experimental works mentioned in Table 11

Table 11 Results from previous works and qualitative comparison with those of present work

Explanation of the problem	Authors	Method employed	Results obtained that coincide with the present study
With gravity modulation and without nanoparticles (for water layer)	Gresho and Sani [2]	Numerical	At low modulated frequency the effect of gravity modulation is to diminish the heat transfer
With gravity modulation and without nanoparticles (for air layer)	Swaminathan et al. [54]	Experimental	At low modulated frequency the effect of gravity modulation is to stabilize the onset of convection
With top-plate temperature modulation and without nanoparticles (for Helium layer)	Niemela and Donnelly [55]	Experimental	The effect of amplitude is to enhance or diminish heat transport depending on value of frequency
With rotational modulation and without nanoparticles (for Helium layer)	Niemela et al. [56]	Experimental	The effect of time-periodic rotational modulation is to suppress heat transport
Without modulation for water–alumina nanoliquid ($\chi = 0.08$) in rectangular enclosure	Elhajjar et al. [57]	Numerical	$Nu = 1.586$

were done by using low Prandtl number liquids [54–56]. The reason for such a choice of Prandtl number is to retain the liquid layer as thin as possible so that it is easy to do experiment in the presence of modulation. Experimenting in the presence of modulation for a nanoliquid layer is quite a challenging task and is still unattempted one.

Having discussed the results of the paper in the next section, we draw a general conclusion.

Conclusion

Based on the results and their discussion, we now come to the following conclusion:

- Effect of dilute concentration of nanoparticles (nanotubes) in base liquid leads to enhancement in heat transport in both no-modulation and also in the case of the three types of modulation problems.
- In the case of gravity-modulated Rayleigh–Bénard convection in Newtonian liquids and Newtonian nanoliquids, the following results are true:
 - $\overline{Nu}_{nl}^{\delta_2=0} > \overline{Nu}_{nl}^{\delta_2 \neq 0}$.
 - The effect of increasing ω^* is to diminish the heat transport and effect of increasing δ_2 is to enhance the heat transport.
 - ω^* effect on \overline{Nu}_{nl} is more significant than that of δ_2 .
- In the case of boundary temperature-modulated Rayleigh–Bénard convection in Newtonian liquids and Newtonian nanoliquids, we observe the following:

- $\overline{Nu}_{nl}^{\delta_2=0} \approx \overline{Nu}_{nl}^{\delta_2 \neq 0}$ for $\varphi = 0$.
- $\overline{Nu}_{nl}^{\delta_2=0} < \overline{Nu}_{nl}^{\delta_2 \neq 0}$ or $\overline{Nu}_{nl}^{\delta_2=0} > \overline{Nu}_{nl}^{\delta_2 \neq 0}$ for all values of φ and depending on the value of ω^* .
- $\overline{Nu}_{nl}^{\varphi=0} < \overline{Nu}_{nl}^{\varphi \neq 0}$ or $\overline{Nu}_{nl}^{\varphi=0} > \overline{Nu}_{nl}^{\varphi \neq 0}$ depending on the choice of ω^* and φ .

- In the case of rotationally modulated Rayleigh–Bénard convection in Newtonian liquids and Newtonian nanoliquids, we observe the following:

- $\overline{Nu}_{nl}^{\delta_2=0} > \overline{Nu}_{nl}^{\delta_2 \neq 0}$.
- The effect of increasing ω^* and Ta_{nl} is to diminish the heat transport and effect of increasing δ_2 is to enhance the heat transport.
- The influence of ω^* and Ta_{nl} on \overline{Nu}_{nl} is more significantly than that of δ_2 .

- Comparing the three types of modulation considered in the paper, it must be observed that both gravity and rotational modulation problems involve non-static configurations. In the case of temperature modulation, however, the system is static. It appears from the results and the above observations that temperature modulation is best suited to regulate convection and heat transport.

Acknowledgements The authors (CK and PGS) are grateful to the Bangalore University for encouragement and the author (PGS) is thankful to Professor Zhao Yi for financial support to visit his research group for collaborative work. The authors (CK and ZY) acknowledge support from the National Natural Science Foundation of China (NSFC) under Project No. 61573119 and a Fundamental Research Project of Shenzhen under Project Nos. JCYJ20170307151312215

and KQJSCX20180328165509766. The authors are thankful to the Reviewers for their most useful comments.

References

- Gershuni GZ, Zhukhovitskii EM. On parametric excitation of convective instability. *J Appl Math Mech.* 1963;27(5):1197–204.
- Gresho PM, Sani RL. The effects of gravity modulation on the stability of a heated fluid layer. *J Fluid Mech.* 1970;40:783–806.
- Gershuni GZ, Zhukhovitskii EM, Iurkov IS. On convective stability in the presence of periodically varying parameter. *J Appl Math Mech.* 1970;34(3):442–52.
- Davis SH. The stability of time periodic flows. *Ann Rev Fluid Mech.* 1976;8:57–74.
- Biringen S, Peltier LJ. Computational study of 3-D Bénard convection with gravitational modulation. *Phys Fluids A.* 1990;2:279–83.
- Wheeler AA, Mc Fadden GB, Murray BT, Coriell SR. Convective stability in the Rayleigh–Bénard and directional solidification problems: high-frequency gravity modulation. *Phys Fluids A Fluid Dyn (1989–1993).* 1991;3(12):2847–58.
- Siddheshwar PG, Kanchana C. Effect of trigonometric sine, square and triangular wavetype time-periodic gravity-aligned oscillations on Rayleigh–Bénard convection in Newtonian liquids and Newtonian nanoliquids. *Meccanica.* 2019;54:451–69.
- Siddheshwar PG, Meenakshi N. Comparison of the effects of three types of time-periodic body force on linear and non-linear stability of convection in nanoliquids. *Eur J Mech B/Fluids.* 2019;77:221–9.
- Venezian G. Effect of modulation on the onset of thermal convection. *J Fluid Mech.* 1969;35:243–54.
- Rosenblat S, Herbert DM. Low-frequency modulation of thermal instability. *J Fluid Mech.* 1970;43(02):385–98.
- Rosenblat S, Tanaka GA. Modulation of thermal convection instability. *Phys Fluids.* 1971;14(7):1319–22.
- Ahlers G, Hohenberg PC, Lücke M. Externally modulated Rayleigh–Bénard convection: experiment and theory. *Phys Rev Lett.* 1984;53(1):48–51.
- Schmitt S, Lücke M. Amplitude equation for modulated Rayleigh–Bénard convection. *Phys Rev A.* 1991;44(8):4986–5002.
- Siddheshwar PG, Bhadauria BS, Suthar OP. Synchronous and asynchronous boundary temperature modulations of Bénard–Darcy convection. *Int J Nonlinear Mech.* 2013;49:84–9.
- Singh J, Singh SS. Instability in temperature modulated rotating Rayleigh–Bénard convection. *Fluid Dyn Res.* 2013;46(1):015504-1-18.
- Chandrasekhar S. *Hydrodynamic and hydromagnetic stability.* Oxford: Clarendon Press; 1961.
- Bhattacharjee JK. Convective instability in a rotating fluid layer under modulation of the rotating rate. *Phys Rev A.* 1990;41:5491–4.
- Küppers G, Lortz D. Transition from laminar convection to thermal turbulence in a rotating fluid layer. *J Fluid Mech.* 1969;35(03):609–20.
- Heikes KE, Busse FH. Weakly nonlinear turbulence in a rotating convection layer. *Ann N Y Acad Sci.* 1980;357(1):28–36.
- Niemela JJ, Donnelly RJ. Direct transition to turbulence in rotating Bénard convection. *Phys Rev Lett.* 1986;57(20):2524–7.
- Geurts BJ, Kunnen RPJ. Intensified heat transfer in modulated rotating Rayleigh–Bénard convection. *Int J Heat Fluid Flow.* <https://doi.org/10.1016/j.ijheatfluidflow.2014.04.007>.
- Kooij GL, Botchev MA, Geurts BJ. Direct numerical simulation of Nusselt number scaling in rotating Rayleigh–Bénard convection. *Int J Heat Fluid Flow.* 2015;55:26–33.
- Choi SUS. *Nanofluid technology: current status and future research,* Korea U.S. Technical Conference on Strategical Technologies, Vienna, V.A. 1998.
- Azmi W, Sharma K, Mamat R, Najafi G, Mohamad M. The enhancement of effective thermal conductivity and effective dynamic viscosity of nanofluids: a review. *Renew Sustain Energy Rev.* 2016;53:1046–58.
- Pinto RV, Fiorelli FAS. Review of the mechanisms responsible for heat transfer enhancement using nanofluids. *Appl Therm Eng.* 2016;108:720–39.
- Esfahani JA, Feshalami BF. Theoretical study of nanofluids behavior at critical Rayleigh numbers. *J Therm Anal Calorim.* 2018. <https://doi.org/10.1007/s10973-018-7582-3>.
- Yadav D, Agrawal S, Bhargava R. Thermal instability of rotating nanofluid layer. *Int J Eng Sci.* 2011;49(11):1171–84.
- Bhadauria BS, Agarwal S. Natural convection in a rotating nanofluid layer. *MATEC Web Conf.* 2012;1:600-1-5.
- Siddheshwar PG, Kanchana C, Kakimoto Y, Nakayama A. Steady finite-amplitude Rayleigh–Bénard convection in nanoliquids using a two-phase model: theoretical answer to the phenomenon of enhanced heat transfer. *ASME J Heat Transf.* 2017;139(1):0124012.
- Siddheshwar PG, Kanchana C, Kakimoto Y, Nakayama A. Study of heat transport in Newtonian water-based nanoliquids using two-phase model and Ginzburg–Landau approach. In: *Proceedings of Vignana Bharathi Golden Jubilee, vol 1, no. 2.* Bangalore University; 2017. p. 93–110. ISSN: 0971-6882.
- Siddheshwar PG, Kanchana C. Unicellular unsteady Rayleigh–Bénard convection in Newtonian liquids and Newtonian nanoliquids occupying enclosures: new findings. *Int J Mech Sci.* 2017;131:1061–72.
- Siddheshwar PG, Kanchana C. A study of unsteady, unicellular Rayleigh–Bénard convection of nanoliquids in enclosures using additional modes. *J Nanofluids.* 2018;7:791–800.
- Akbarzadeh P. The onset of MHD nanofluid convection between a porous layer in the presence of purely internal heat source and chemical reaction. *J Therm Anal Calorimetry.* 2017. <https://doi.org/10.1007/s10973-017-6710-9>.
- Siddheshwar PG, Lakshmi KM. Unsteady finite amplitude convection of water–copper nanoliquid in high porosity enclosures. *ASME J Heat Transf.* 2019;141:062405-1–11.
- Siddheshwar PG, Lakshmi KM. Darcy–Bénard convection of Newtonian liquids and Newtonian nanoliquids in cylindrical enclosures and cylindrical annuli. *Phys Fluids.* 2019;31(7):084102.
- Wikipedia contributors, Thermoacoustic heat engine. https://en.wikipedia.org/w/index.php?title=Thermoacoustic_heat_engine&oldid=920708336.
- Bodenschatz E, Pesch W, Ahlers G. Recent developments in Rayleigh–Bénard convection. *Ann Rev Fluid Mech.* 2000;32:709–78.
- Kanchana C, Siddheshwar PG. Transforming analytically intractable dynamical systems with a control parameter into a tractable Ginzburg–Landau equations: few illustrations. *Napal Math Soc Rep.* 2019;35:35–44.
- Brinkman HC. The viscosity of concentrated suspensions and solutions. *J Chem Phys.* 1952;20(4):571.
- Hamilton RL, Crosser OK. Thermal conductivity of heterogeneous two-component systems. *Ind Eng Chem Fundam.* 1962;1(3):187–91.
- Buongiorno J. Convective transport in nanofluids. *ASME J Heat Transf.* 2006;128(3):240–50.
- Siddheshwar PG. A series solution for the Ginzburg–Landau equation with a time-periodic coefficient. *Appl Math.* 2010;1(06):542–54.
- Kanchana C, Zhao Y. Effect of internal heat generation/absorption on Rayleigh–Bénard convection in water well-dispersed

- with nanoparticles or carbon nanotubes. *Int J Heat Mass Transf.* 2018;127:1031–47.
44. [link]. <http://www.us-nano.com>.
 45. Corcione M. Rayleigh–Bénard convection heat transfer in nanoparticle suspensions. *Int J Heat Fluid Flow.* 2011;32(1):65–77.
 46. Paramethanuwat T, Bhuwakietkumjohn N, Rittidech S, Ding Y. Experimental investigation on thermal properties of silver nanofluids. *Int J Heat Fluid Flow.* 2015;56:80–90.
 47. Xuan Y, Li Q. Heat transfer enhancement of nanofluids. *Int J Heat Fluid Flow.* 2000;21:58–64.
 48. Dang TMD, Le TTT, Fribourg-Blanc E, Dang MC. The influence of solvents and surfactants on the preparation of copper nanoparticles by a chemical reduction method. *Adv Nat Sci Nanosci Nanotechnol.* 2011;2:025004-1-9.
 49. Khanafer K, Vafai K, Lightstone M. Buoyancy-driven heat transfer enhancement in a two-dimensional enclosure utilizing nanofluids. *Int J Heat Mass Transf.* 2003;46(19):3639–53.
 50. Jou RY, Tzeng SC. Numerical research of nature convective heat transfer enhancement filled with nanofluids in rectangular enclosures. *Int Commun Heat Mass Transf.* 2006;33(6):727–36.
 51. Abu-Nada E, Masoud Z, Hijazi A. Natural convection heat transfer enhancement in horizontal concentric annuli using nanofluids. *Int Commun Heat Mass Transf.* 2008;35(5):657–65.
 52. Siddheshwar PG, Meenakshi N. Amplitude equation and heat transport for Rayleigh–Bénard convection in Newtonian liquids with nanoparticles. *Int J Appl Comput Math.* 2015;2:1–22.
 53. Kanchana C, Zhao Y, Siddheshwar PG. A comparative study of individual influences of suspended multiwalled carbon nanotubes and alumina nanoparticles on Rayleigh–Bénard convection in water. *Phys Fluids.* 2018;30:084101.
 54. Swaminathan A, Garrett SL, Poese ME, Smith RWM. Dynamic stabilization of the Rayleigh–Bénard instability by acceleration modulation. *J Acoust Soc America.* 2018;144:2334–43.
 55. Niemela JJ, Donnelly RJ. External modulation of Rayleigh–Bénard convection. *Phys Rev Lett.* 1987;59:2431–4.
 56. Niemela JJ, Smith MR, Donnelly RJ. Convective instability with time-varying rotation. *Phys Rev A.* 1991;44:8406–9.
 57. Elhajjar B, Bachir G, Mojtabi A, Fakhri C, Charrier-Mojtabi MC. Modeling of Rayleigh–Bénard natural convection heat transfer in nanofluids. *C R Mécanique.* 2010;338(6):350–4.
 58. Kanchana C, Siddheshwar PG, Zhao Yi. A study of Rayleigh–Bénard convection in hybrid nanoliquids with physically realistic boundaries. *Eur Phys J Spec Topic.* 2019;228:2511–30.
 59. Siddheshwar PG, Shivakumar BN, Zhao Yi, Kanchana C. Rayleigh–Bénard convection in Newtonian liquids bounded by rigid isothermal boundaries. *Appl Math Comput.* 2019;371:124942.

Publisher's Note Springer Nature remains neutral with regard to jurisdictional claims in published maps and institutional affiliations.